

# Quality Not Quantity: On the Interaction between Dataset Design and Robustness of CLIP

Thao Nguyen<sup>1</sup>      Gabriel Ilharco<sup>1</sup>      Mitchell Wortsman<sup>1</sup>  
 Sewoong Oh<sup>1</sup>      Ludwig Schmidt<sup>1,2</sup>

## Abstract

Web-crawled datasets have enabled remarkable generalization capabilities in recent image-text models such as CLIP (Contrastive Language-Image pre-training) or Flamingo, but little is known about the dataset creation processes. In this work, we introduce a testbed of six publicly available data sources—YFCC, LAION, Conceptual Captions, WIT, RedCaps, Shutterstock—to investigate how pre-training distributions induce robustness in CLIP. We find that the performance of the pre-training data varies substantially across distribution shifts, with no single data source dominating. Moreover, we systematically study the interactions between these data sources and find that combining multiple sources does not necessarily yield better models, but rather dilutes the robustness of the best individual data source. We complement our empirical findings with theoretical insights from a simple setting, where combining the training data also results in diluted robustness. In addition, our theoretical model provides a candidate explanation for the success of the CLIP-based data filtering technique recently employed in the LAION dataset. Overall our results demonstrate that simply gathering a large amount of data from the web is not the most effective way to build a pre-training dataset for robust generalization, necessitating further study into dataset design. Code is available at [https://github.com/mlfoundations/clip\\_quality\\_not\\_quantity](https://github.com/mlfoundations/clip_quality_not_quantity).

## 1 Introduction

Large models pre-trained on web-scale datasets are becoming a cornerstone of machine learning. For instance, the past two years have witnessed the arrival of several new models such as GPT-3 [12], Chinchilla [37], and PaLM [15] for natural language processing, or CLIP [61], BASIC [58], and Flamingo [3] for computer vision. These models exhibit unprecedented generalization capabilities in zero-shot inference, in-context learning, and robustness to distribution shift. A key ingredient enabling their generalization performance are the large and diverse pre-training corpora that exceed previous datasets by multiple orders of magnitude. For instance, the training set of BASIC [58] contains 6.6 billion images, which is more than 1,000 times larger than the widely used ImageNet [19] training set from the 2012 competition containing 1.2 million images.

Despite the central role datasets play for pre-trained models, little is known about them, especially for image-text models. The aforementioned CLIP [61], BASIC [58], and Flamingo [3] all rely on datasets internal to the respective organizations, which is also the case for other models such as DALL-E [63],

<sup>1</sup>University of Washington {thaottn, gamaga, mitchnw, sewoong, schmidt}@cs.washington.edu

<sup>2</sup>Allen Institute for Artificial Intelligence

Florence [86], and ALIGN [39]. In addition, research publications often provide little details on the data collection processes, e.g., the data sources or data filtering mechanisms. Beyond clear issues such as reproducibility and the potential presence of harmful content, the opaque dataset creation practices also make it hard to identify effective methods for assembling pre-training datasets. As a result, researchers cannot build on each other’s dataset innovations, which obstructs the incremental research process that has successfully accumulated algorithm and architecture improvements in machine learning models. A more principled understanding of dataset creation will likely enable further progress in the generalization capabilities of pre-trained models.

A basic approach to dataset creation would be to simply train on *all* available data of a given type. While scaling up training sets has indeed been integral to the recent progress in large models, advances in weak and self-supervision [12, 14, 21, 33, 34] have led to an abundance of potential training data. For instance, the large LAION-5B dataset [2] of 5 billion image-text pairs is itself a subset of about 50 billion images from Common Crawl. This abundance is already exceeding the amount of data models can currently be trained on within a reasonable time,<sup>1</sup> making the aforementioned baseline of using all available data infeasible. Consequently, deciding *what* data to train on is becoming increasingly important.

In this paper, we take a step towards a better understanding of pre-training data and investigate the impact of dataset design on the generalization capabilities of image-text models. Specifically, we focus on CLIP, the first large model of this kind that demonstrated remarkable robustness to multiple challenging distribution shifts. The main questions we ask are: (i) How much do different web data sources vary in their induced robustness? (ii) Do dataset combinations lead to better robustness? (iii) Can filtering with an existing image-text model improve data quality? We address these questions from both an experimental and theoretical perspective.

On the experimental side, we begin by assembling a corpus of six different datasets from the web, spanning a variety of sources including Flickr, Shutterstock, Wikipedia, Common Crawl, and Reddit. We then measure the robustness of CLIP models trained on each dataset. In particular, we compare the zero-shot accuracy of these models on ImageNet and a set of canonical ImageNet distribution shifts. We find that the robustness induced by each pre-training dataset varies widely, and that sources with careful curation such as Wikipedia do not necessarily outperform those with minimal filtering.

In addition, the datasets cannot be compared along a single dimension: different datasets help with robustness to different distribution shifts. This in turn motivates studying how combining datasets affects robustness. We find that a model trained on two datasets does not inherit the robustness properties of both. Rather, while the model is exposed to both distributions, its robustness interpolates between that of the individual datasets. This indicates that dataset designers must carefully combine the pre-training data in order to preserve and enhance the robustness of the resulting models.

Building on our empirical results, we introduce a theoretical model to better understand our experimental findings. Our model is simple enough to allow for mathematical analysis and can still capture some phenomena of real-world, web-crawled datasets. Specifically, our theoretical model also shows that combining multiple datasets dilutes the robustness of the better data distribution.

---

<sup>1</sup>Recall that the training set for Google’s largest image-text model ALIGN contains “only” 6.6 billion images, making it about eight times smaller than the source dataset for LAION-5B.

Moreover, our model provides a candidate explanation for another interesting phenomenon in the curation of pre-training data: the LAION-400M experiment [68] and follow-up CLIP reproductions [2] demonstrated that filtering a noisy source (Common Crawl) with a CLIP model results in a dataset on which newly trained CLIP models exhibit *higher* robustness to some distribution shifts.

**Paper outline.** We first briefly review related work and the relevant background on robustness to distribution shift (Section 2), before discussing our experimental setup in Section 3. Sections 4 and 5 then measure the robustness of CLIP induced by individual data sources and their combinations. To support these empirical results, Section 6 presents our theoretical analysis. We conclude with future research directions in Section 7.

## 2 Background & Related Work

**Vision-language models.** Large vision-language models like CLIP and ALIGN have become an active area of research owing to their success on various computer vision tasks [39, 61]. Existing work expands their capabilities by either increasing model and dataset size [58], or by using additional supervision as in DeCLIP [46], SLIP [54], and FILIP [84]. In contrast, we study the effect of *pre-training data composition* on task performance with a focus on robustness.

In a recent work, Fang et al. [24] showed that CLIP’s robustness primarily stems from its diverse pre-training distribution and not training set size, language supervision, or contrastive loss functions. However, Fang et al. [24] only conducted experiments with two datasets (YFCC-15M and ImageNet-Captions), one of which contains less than one million images. We take the insights of Fang et al. [24] as our starting point and expand the range of pre-training datasets to six different sources, each containing at least five million images. This enables us to study the robustness induced by various pre-training sources, and how dataset combinations affect robustness.

**Distribution shift.** Robustness to distribution shift is a long-standing issue in machine learning [60, 78] and has recently received renewed attention as researchers scrutinize the generalization performance of neural networks in greater detail [5, 8, 9, 16, 31, 44, 66, 74]. Similar to CLIP [61], we focus on robustness to natural distribution shifts, where the corresponding test sets contain only unmodified images and are not intentionally perturbed by adversarial examples or synthetic corruptions (such as Gaussian noise or blur patterns) [35]. Specifically, we test robustness on ImageNetV2 [65], ImageNet-R [36], ImageNet-Sketch [81], and ObjectNet [6] because prior work has established many baselines for these distribution shifts [75]. Moreover, models robust to these shifts also show improved robustness on other out-of-distribution benchmarks such as WILDS [42, 82].

The robustness literature usually discusses distribution shift in terms of “in-distribution” and “out-of-distribution”

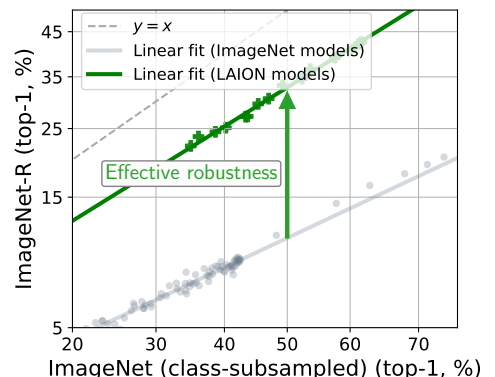


Figure 1: Models pre-trained on LAION exhibit *effective robustness* [75] compared to standard models trained on ImageNet. Effective robustness is defined as movement towards a classifier which is robust to distribution shift. A classifier is more robust the closer it is to the  $y = x$  line. A classifier on the  $y = x$  line is not affected by the distribution shift.

data. This terminology is natural when data from the same distribution as the “in-distribution” test set is used for training or fine-tuning. However, it is unclear what counts as “in-distribution” when models are trained on large-scale, generic pre-training datasets that aim to improve performance on a wide variety of tasks. To address this issue, we follow the more flexible definition of distribution shift employed in prior work [52, 75] and measure robustness as accuracy difference between two related but distinct test distributions (e.g., ImageNet and ImageNet-Sketch). The expectation is that the shift between the two test distributions should not affect an ideal robust model, for instance because the shift does not affect the accuracy of humans labelers [69]. Taori et al. [75] defined this notion of robustness as *effective robustness*. Radford et al. [61] adopted the effective robustness framework in the evaluations of their CLIP model. Effective robustness is illustrated in Figure 1 and measures movement towards a perfectly robust classifier which is not affected by the shift between two test distributions.

Prior work [52] has evaluated several hundred models and demonstrated experimentally that changes to model architecture, training set size, training algorithm, and other model-related factors do *not* change effective robustness in most cases. In contrast, changes to the pre-training *distribution* can improve the effective robustness of a model. This makes effective robustness a useful metric for evaluating the influence of pre-training data sources on robust generalization, since it removes confounders stemming from model hyperparameters and the number of training samples. The effect of the pre-training distribution on effective robustness is particularly pronounced when models are evaluated in a zero-shot setting: while training on a target distribution can improve accuracy on that distribution [28, 82, 83, 87, 88], this process can deteriorate robustness to distribution shift [4, 58, 61, 82].

The existence of a universal linear trend for accuracies on a pair of test sets has been analytically studied in [52]. For a simple binary classification model similar to our Assumption 1 (see Section 6), convergence to a linear trend is shown with the deviation from the line scaling as  $O(1/\sqrt{d})$ . However, the analysis in [52] is restricted to a specific stochastic distribution shift for the out-of-distribution test data and a fixed classifier independent of the training data. Hence the dependence of the slope on the training set size, variations in the training methods, and properties of the training distribution cannot be described in their model. We provide significantly more fine-grained analyses (Theorem 1) that captures all such tradeoffs, which allows us to draw novel insights into how data mixing (Theorem 2) and filtering (Theorem 3) affect model robustness.

### 3 Experiment Setup

**Model.** We focus on the CLIP model [61] which has demonstrated unprecedented zero-shot performance on a wide range of downstream tasks, as well as robustness to various distribution shifts [52]. Given an image-text pair, CLIP is trained to maximize the cosine similarity between the embedding of the text and that of the image, relative to the similarity of unconnected image-text pairs. We use the CLIP implementation from the OpenCLIP GitHub repository [38], with ResNet-50 [32] as the image encoder architecture. We vary the pre-training set size and hyperparameters such as number of epochs to obtain different accuracies on each data distribution. Due to compute constraints, the total training set size is at most 15M samples for most of our experiments. Appendix B contains further training details.

**Data.** To study the effects of training distributions on robust generalization, we collect several

datasets from publicly available sources. Most of these have been studied in the context of various vision and language tasks in previous work:

- YFCC: We experiment with the 15M subset of the YFCC100M dataset [76] that the original CLIP paper [61] used for dataset ablation studies. The images and captions are collected from Flickr.
- LAION [68]: The images and corresponding alt-texts come from web pages collected by Common Crawl [1] between 2014 and 2021. We randomly select a subset of 15M samples to experiment with, and ensure that the accompanying NSFW tags of all chosen images are ‘UNLIKELY’.
- Conceptual Captions [13]: We use CC-12M for our experiments, which consists of images and HTML alt-text from an unspecified set of web pages.
- RedCaps [20]: This dataset contains 12M examples, obtained from 350 manually curated subreddits between 2008 and 2020. The subreddits are selected to contain a large number of image posts that are mostly photographs and not images of people.
- Shutterstock: 15M images and captions were crawled from the Shutterstock website in 2021.
- WIT [71]: Image-text pairs come from Wikipedia pages. We use reference description as the source of text data and obtain 5M examples in total after filtering to include only English language examples.

Appendix A.1 contains an analysis of image and text statistics, as well as randomly selected data samples from each source.

**Evaluation.** Similar to Taori et al. [75] and Radford et al. [61], we choose ImageNet as the reference distribution and evaluate CLIP on four natural distribution shifts derived from ImageNet:

- ImageNet-V2 [65]: A reproduction of the ImageNet validation set closely following the original dataset creation process.
- ImageNet-R [36]: Renditions (e.g., sculptures, paintings, etc.) for 200 ImageNet classes.
- ImageNet-Sketch [81]: Sketches of ImageNet class objects.
- ObjectNet [6]: A test set of objects in novel backgrounds, rotations, and viewpoints with 113 classes overlapping with ImageNet

Visualizations of random samples from each distribution shift can be found in Appendix A.2.

## 4 Individual Pre-training Data Sources

We first investigate how well a CLIP model trained on each data source would perform under different distribution shifts of interest. As seen from Figure 2, while all sources yield the same linear trend on ImageNet-V2, some display clear advantages when evaluated on other test distributions. For example, Shutterstock offers the best out-of-distribution performance on ImageNet-Sketch, while RedCaps displays the most effective robustness on ObjectNet. On ImageNet-R, LAION, CC12M and Shutterstock seem to do much better than the rest. Overall no pre-training data distribution is consistently the most robust across all evaluation settings.

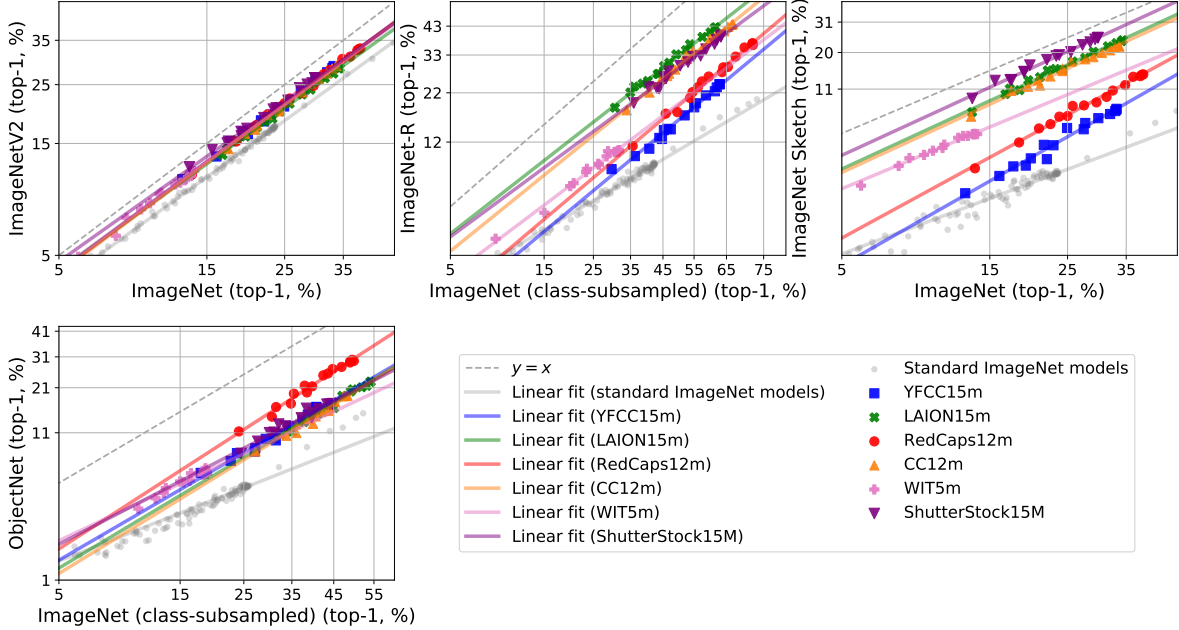


Figure 2: **Performance of the six pre-training data sources under various distribution shifts.** We find that the behavior—both in terms of accuracy and the slope of the linear trend—of the pre-training data varies substantially across distribution shifts, with no single data source dominating. Most shifts help highlight the strengths and weaknesses of different data sources, except for ImageNet-V2, where the linear trends produced by individual sources are highly correlated with one another.

We also measure the data efficiency of each source, i.e., how much the performance would change with more samples from the same source, see Appendix C. Similar to the previous observation, the six pre-training sources display vastly different data efficiency depending on the distribution shifts of interest. Although LAION and CC-12M exhibit similar effective robustness in all evaluation settings in Figure 2, this analysis reveals subtle differences between these two training distributions in the low-data regimes.

## 5 Combining Data Sources

In the previous section, we demonstrate the variability in behavior of different data sources based on the distribution shift at test time. A natural question then arises from this observation: does combining multiple sources help improve robustness across some, if not all, test distributions of interest? We investigate two common approaches of aggregating information from different training sets—input mixing and output ensembling. In the subsequent discussion, we focus on distribution shifts that bring out significant differences in behavior across the pre-training data sources (e.g., ImageNet-R and ImageNet-Sketch); the full results on all distribution shifts can be found in Appendices D and E.



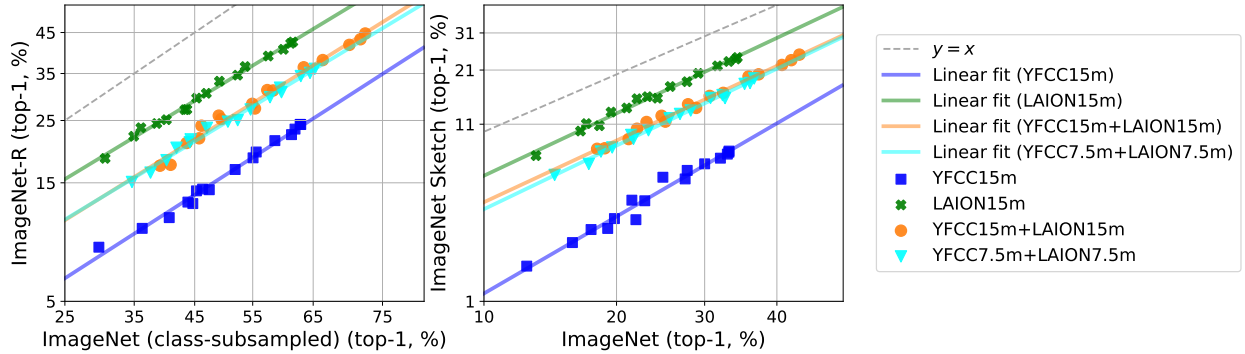


Figure 3: **Combining YFCC and LAION training data in equal ratios produces models with intermediate robustness.** Given a fixed data budget of 15M samples, the linear trend produced by training CLIP on a YFCC-LAION data mixture, with 7.5M datapoints from each source (cyan line), lies between that of training CLIP on YFCC (blue line) and LAION (green line) entirely. Even when we increase the total training set size (30M) and use all data available from both sources (orange line), the same pattern persists.

## 5.1 Input Mixing

In input mixing, we randomly select and combine samples from multiple data sources to build the pre-training dataset. Our findings indicate that this exposure to more training distributions doesn’t help CLIP take advantage of the complimentary strengths of each source. Rather, the effective robustness of the resulting model is less than that of training on the best individual source for each distribution shift.

We start with combining data from two largest data sources in the testbed—YFCC and LAION. To remove dataset size as a confounder, we fix the total amount of training data at 15M samples, and sample 7.5M image-text pairs from each source. This data mixture yields a linear trend that lies in between the trends obtained from training on 15M YFCC and 15M LAION datapoints separately (Figure 3). Even when we remove the constraint on the training set size and use all the data available from these two sources (i.e., 30M samples), the same observation on robustness holds, and the resulting linear trend is highly correlated with that of training on the YFCC-7.5M + LAION-7.5M mixture.

The previous set of experiments combines YFCC and LAION data with a 50:50 ratio. In Figure 4, we find that when this ratio is varied within a fixed budget of 15M datapoints, the robustness linear trends of the corresponding mixtures form a smooth interpolation between the linear trends of training on 15M YFCC and 15M LAION samples separately. Experiments with different combinations of sources, as well as mixtures of a larger number of sources, can be found in Appendix D. There we also include results for combining data from CIFAR-10 and CINIC-10 distributions to train ResNets on image classification tasks, where we observe the same interpolation pattern. We provide a theoretical justification for this phenomenon in Section 6.2.

## 5.2 Output Mixing

Another common approach to take advantage of different training sets is to combine them at model output level (i.e., ensemble) [7, 11, 22, 25, 26, 29, 45, 56]. Here, we train a CLIP model on each

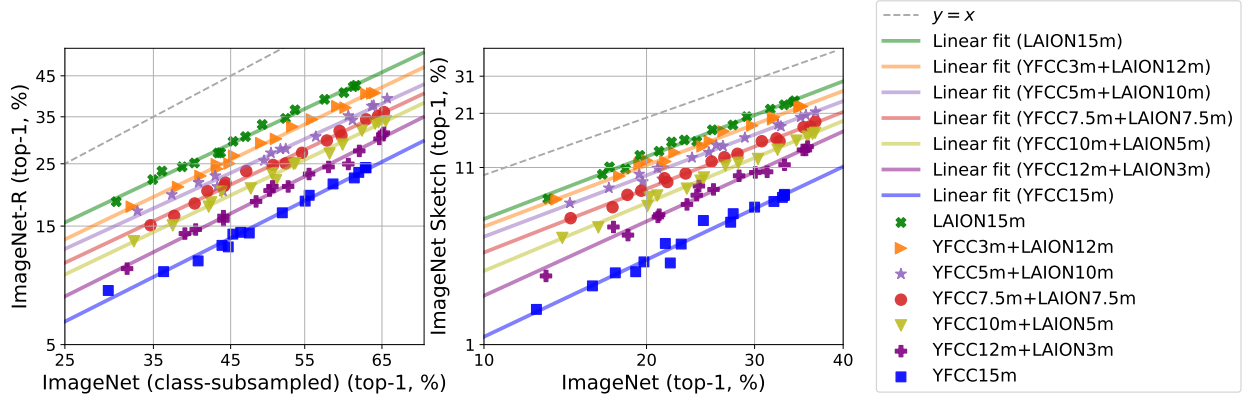


Figure 4: **Varying the sample contributions of YFCC and LAION to the input data mixture produces a smooth interpolation of the linear trend between those of training on YFCC and LAION separately.** Keeping the total number of training samples fixed at 15M, as we vary the contribution of YFCC to the dataset mixture from 15M (i.e., only training on YFCC) to 0M (i.e., only training on LAION), the resulting linear trend gradually shifts from that of YFCC-15M (blue line) to that of LAION-15M (green line).

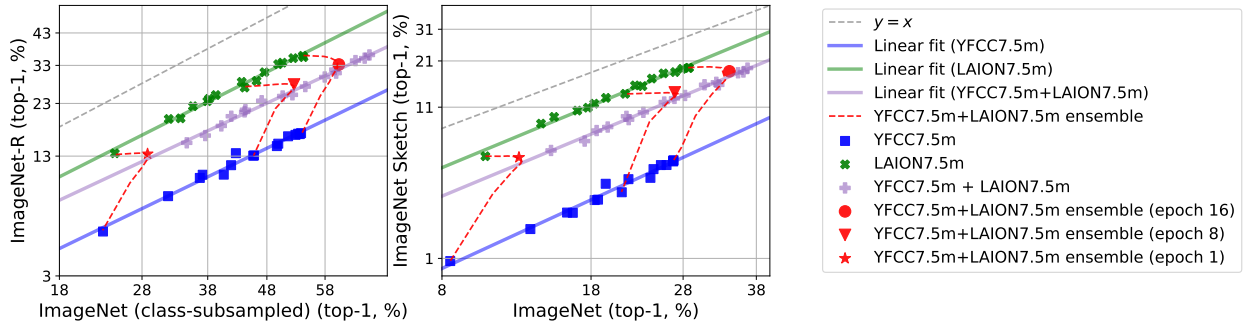


Figure 5: **Ensemble outputs of CLIP models trained on YFCC and LAION separately share the same linear trend as a single model trained on the combined data mixture (where each source contributed equally).** We ensemble the logit predictions of YFCC-trained (blue line) and LAION-trained (green line) models taken from the same epoch, with varying ensemble weights between 0 and 1 (red dashed line). When the outputs are combined with equal weights (red markers), the resulting test accuracies closely track the linear trend produced by pre-training CLIP on a data mixture with equal number of samples from each source (purple line).



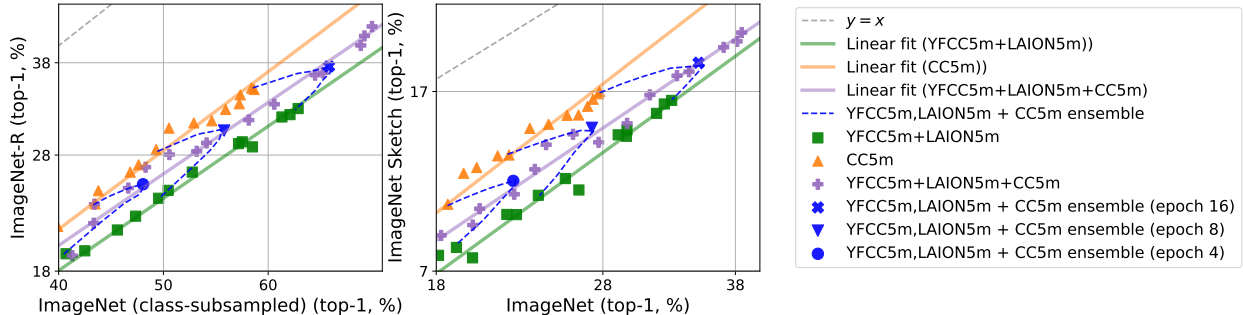


Figure 6: **Using ensemble outputs to predict the linear trend of input mixing without retraining CLIP from scratch.** A generalization of the observation made in Figure 5 is that given an existing pre-training dataset that could be a mixture (e.g., YFCC-5M + LAION-5M, green line) and a new data source (e.g., CC-5M, orange line), we could use the ensemble outputs (blue markers) of two CLIP models that have been trained separately on these two data distributions, to estimate where the linear trend for a CLIP model trained on *all* the data would lie (purple line). This removes the need to actually train CLIP from scratch on the now bigger 3-source mixture.

pre-training distribution of interest and combine the logit predictions of all the resulting models with equal weights. In experiments with mixing YFCC and LAION (Figure 5), the ensembles of 2 single-source-trained CLIP models taken from the same epoch of training, lie on the linear trend of a *single* CLIP model trained on the combined data. This holds across different distribution shifts that we consider. The same observation also applies when we ensemble 6 CLIP models trained separately on the 6 data sources collected, with the contribution of each model being weighted equally. Refer to Appendix E for more details.

We next show that this phenomenon extends to more complex mixtures. The fact that output mixing (i.e., ensembling the predictions of CLIPs trained on individual sources) is predictive of the linear trend produced by input mixing (i.e., training on *all* the data from these sources) presents an opportunity to estimate model robustness given new data sources, without having to train the model from scratch on the new, potentially much larger, combined dataset. For example, in Figure 6, assuming access to a CLIP model trained on the YFCC-5M + LAION-5M mixture, and another one trained on CC-5M, the ensembles of these two models across different stages of training share the same linear trend as a CLIP model trained on the YFCC-5M + LAION-5M + CC-5M mixture. In Appendix E, we show the results of ensembling 6 CLIP models trained with the 6 data sources we collected, as well as the CINIC-10 + CIFAR-10 ensemble, a uni-modal image classification setting where output mixing accuracies are also predictive of the linear trend of input mixing.

## 6 Analysis under Simple Binary Classification Models

Empirically we observe, for e.g., in Figure 2, that for a pair of test datasets ( $\mathcal{D}_1, \mathcal{D}_2$ ), the corresponding test accuracies after probit transform achieved by various trained models (including different architectures and training algorithms) on the same training dataset  $\mathcal{D}$  all lie on the same line. Furthermore, this line includes models trained on only a subset of  $\mathcal{D}$  [52]. In other words, there is a universal line that is determined only by the training data distribution and the two test distributions, and is independent of which architecture we use, how we train the model, or how many samples

we use from the training set. To explain this phenomenon, we study the following class of trained models parametrized by  $(\theta \in \mathbb{R}^d, \rho \in \mathbb{R}_+)$  representing the training distribution, with  $n$  representing the training data size, and  $\xi \in \mathbb{R}_+$  representing the variations due to the training algorithm.

## 6.1 Universality of Accuracy on the Line for Binary Classification

We analyze a simple but canonical binary classification example where each training data is parametrized by its ground-truth linear classifier  $\theta \in \mathbb{R}^d$  and its Signal-to-Noise Ratio (SNR)  $\rho^2 \in \mathbb{R}_+$ . Concretely, a training dataset  $\mathcal{D}_{n,\theta,\rho} = \{(x_i \in \mathbb{R}^d, y_i \in \pm 1)\}_{i=1}^n$  is a set of  $n$  i.i.d. paired samples from a joint distribution  $P_{\theta,\rho}$  defined as follows.

**Assumption 1** (Data distribution). *We define a joint distribution  $(x_i, y_i) \sim P_{\theta,\rho}$  as (i)  $y_i = \pm 1$  uniformly at random, and (ii)  $x_i = y_i\theta + (\|\theta\|/\rho)z_i$  where the noise  $z_i$  is zero-mean and has independent entries with variance one. For an observation  $(x_i, y_i)$ , we refer to  $\|\theta\|^2$  as the signal power and  $\|\theta\|^2/\rho^2$  as the corresponding noise power with SNR  $\rho^2$ .*

**Assumption 2** (Trained model distribution). *We consider a (random) linear model parameter  $\hat{\theta}_{n,\xi} \in \mathbb{R}^d$  that predicts a binary label  $\text{sign}(\langle x, \hat{\theta}_{n,\xi} \rangle)$  for a test example  $x \in \mathbb{R}^d$ . We assume that the random model  $\hat{\theta}_{n,\xi} = \theta + (\xi\|\theta\|/(\rho\sqrt{n}))z \in \mathbb{R}^d$ , trained on  $\mathcal{D}_{n,\theta,\rho}$  is unbiased,  $\mathbb{E}[\hat{\theta}_{n,\xi}] = \theta$ , and that  $z$  has independent entries with variance one each. The randomness comes from the training data as well as any internal randomness in the training algorithm. The parameter  $\xi \in \mathbb{R}_+$  captures the variations in the resulting model distribution due to changes the training algorithm.*

Concretely, one canonical example of a trained model is  $\hat{\theta}_{n,\xi} = (1/n) \sum_{i=1}^n y_i x_i$ . It follows that  $\hat{\theta}_n = \theta + (\|\theta\|/(\rho\sqrt{n}))z$  with  $\xi = 1$ . Hence,  $\xi$  measures the randomness of the trained model relative to this simple training algorithm.

We analyze the resulting accuracy when evaluated on two test distributions  $P_{\theta_1,\rho_1}$  and  $P_{\theta_2,\rho_2}$  as defined above, with  $\text{Acc}_{\theta_1,\rho_1} := P_{\theta_1,\rho_1}\{\text{sign}(\langle X, \hat{\theta}_{n,\xi} \rangle) = Y\}$ , and  $\text{Acc}_{\theta_2,\rho_2}$  defined similarly. In particular, we are interested in how the accuracy pair  $(\Phi^{-1}(\text{Acc}_{\theta_1,\rho_1}), \Phi^{-1}(\text{Acc}_{\theta_2,\rho_2}))$  behaves as we vary the sample size  $n$  and as we vary the training algorithm represented by  $\xi$ . Here,  $\Phi^{-1} : [0, 1] \rightarrow \mathbb{R}$  is the inverse of the CDF of a standard Gaussian distribution, defined as  $\Phi(t) = \mathbb{P}(z \leq t)$  where  $z \sim \mathcal{N}(0, 1)$ .  $\Phi^{-1}$  is also called the probit function. This choice of mapping the accuracy with the probit function is critical in getting the linear relation, which we will explain in Remark 1.

**Theorem 1** (Universality of accuracy on the line). *Under Assumptions 1 and 2, asymptotically as the dimension  $d$  grows linearly in the sample size  $n$  such that  $\lim_{d \rightarrow \infty} n/d = \alpha^2$ , we have*

$$\lim_{d \rightarrow \infty} \text{Acc}_{\theta_1,\rho_1} = \Phi\left(\cos(\theta_1, \theta) \frac{\rho_1 \rho^\alpha}{\xi}\right), \text{ and } \lim_{d \rightarrow \infty} \text{Acc}_{\theta_2,\rho_2} = \Phi\left(\cos(\theta_2, \theta) \frac{\rho_2 \rho^\alpha}{\xi}\right). \quad (1)$$

Further, under Assumption 5 in the Appendix, for some universal constant  $c > 0$ ,

$$\Phi^{-1}(\text{Acc}_{\theta_2,\rho_2}) = \frac{\cos(\theta_2, \theta) \rho_2}{\cos(\theta_1, \theta) \rho_1} \Phi^{-1}(\text{Acc}_{\theta_1,\rho_1}) + O\left(\frac{e^{\frac{cn}{d}}}{\sqrt{n}}\right). \quad (2)$$

We provide a proof in Appendix F.1. This analysis implies that for any training sample size  $n$  and any (variation due to the) training algorithm  $\xi$ , the resulting accuracy pair after probit transform lies on a *universal* line determined by Eq. (2), and the slope only depends on the two test distributions

$(P_{\theta_1, \rho_1}, P_{\theta_2, \rho_2})$  and the training distribution  $P_{\theta, \rho}$ . The similarity between the training data and each test dataset is captured by the angles:  $\cos(\theta_1, \theta)$  and  $\cos(\theta_2, \theta)$ . More similar training data achieves a larger test accuracy. The hardness of the test distribution is captured by the SNR of each test dataset:  $\rho_1$  and  $\rho_2$ . We emphasize that this line is universal in the sense that the slope does not depend on the sample size  $n$  and training algorithm parameter  $\xi$ . We are interested in the regime where  $n$  scales linearly in  $d$  and both are large such that the second term in the above equation is negligible.

*Remark 1. Why do we get the accuracy-on-the-line phenomenon?* The prediction of the trained (random) linear model on a random test data point  $X$  involves the inner product, which performs a natural spatial averaging over the  $d$  coordinates. Since the noise across the coordinates is independent and has bounded variance, the central limit theorem applies. The resulting error has a Gaussian tail. Hence, the probit mapping,  $\Phi^{-1}(\text{Acc}_{\theta_1, \rho_1})$ , is critical in translating accuracy into the relevant mean to standard deviation ratio:  $\cos(\theta_1, \theta)\rho_1\rho\sqrt{n}/(\xi\sqrt{d})$ . This is consequently important for getting the universal linear relation, because irrelevant parameters,  $n$  and  $\xi$ , cancel out in the slope of  $\Phi^{-1}(\text{Acc}_{\theta_2, \rho_2})/\Phi^{-1}(\text{Acc}_{\theta_1, \rho_1})$ . Refer to the proof of Theorem 1 (Appendix F.1) for more details.

*Remark 2. Intersection at the random guess:* Previous work [52] that considered models with a wide range of accuracies has found that all lines intersect at a point corresponding to “random guess”, which in this binary example is  $(\Phi^{-1}(1/2), \Phi^{-1}(1/2)) = (0, 0)$ . Our theoretical analysis is consistent with this empirical observation: all universal lines intersect at  $(0, 0)$  up to a small additive error scaling as  $O(1/\sqrt{n})$ .

## 6.2 Input Mixing Yields an Intermediate Slope

Figures 3 and 4 show that when a model is trained on samples combined from two datasets, the resulting robustness trend lies in between the trends achieved by individual datasets. We show that this finding is universally true under our current setup in Theorem 2. Note that for the linear models we consider, input mixing (combining training sets) and output mixing (combining model outputs) are equivalent.

**Assumption 3.** Consider two training datasets  $\mathcal{D}_{n_1, \tilde{\theta}_1, \tilde{\rho}_1}$  and  $\mathcal{D}_{n_2, \tilde{\theta}_2, \tilde{\rho}_2}$  of sizes  $n_1$  and  $n_2$  from distributions  $P_{\tilde{\theta}_1, \tilde{\rho}_1}$  and  $P_{\tilde{\theta}_2, \tilde{\rho}_2}$  as defined in Assumption 1. Separately training on individual datasets gives two models  $\hat{\theta}_{n_1, \xi_1}(\mathcal{D}_{n_1, \tilde{\theta}_1, \tilde{\rho}_1})$  and  $\hat{\theta}_{n_2, \xi_2}(\mathcal{D}_{n_2, \tilde{\theta}_2, \tilde{\rho}_2})$  as defined in Assumption 2. A model trained on a combined (and possibly subsampled) training dataset  $\mathcal{D}_{n'_1, \tilde{\theta}_1, \tilde{\rho}_1} \cup \mathcal{D}_{n'_2, \tilde{\theta}_2, \tilde{\rho}_2}$  is represented by  $\hat{\theta}_{n'_1+n'_2, \xi}(\mathcal{D}_{n'_1, \tilde{\theta}_1, \tilde{\rho}_1} \cup \mathcal{D}_{n'_2, \tilde{\theta}_2, \tilde{\rho}_2}) = \bar{\theta} + (\xi\|\bar{\theta}\|/(\bar{\rho}\sqrt{n'_1+n'_2}))z$  where  $\bar{\theta} = (n'_1\tilde{\theta}_1 + n'_2\tilde{\theta}_2)/(n'_1 + n'_2)$ ,  $\bar{\rho} = \|\bar{\theta}\|/\sqrt{(n'_1\|\tilde{\theta}_1\|^2/\rho_1^2) + (n'_2\|\tilde{\theta}_2\|^2/\rho_2^2)}$ , and  $z \in \mathbb{R}^d$  is a zero-mean random vector with independent entries each with variance one.

Again, a canonical example of a trained model is  $\hat{\theta}_{n'_1+n'_2, \xi} = (1/(n'_1 + n'_2))(\sum_{(x_i, y_i) \in \mathcal{D}_{n'_1, \tilde{\theta}_1, \tilde{\rho}_1}} y_i x_i + \sum_{(x_i, y_i) \in \mathcal{D}_{n'_2, \tilde{\theta}_2, \tilde{\rho}_2}} y_i x_i)$ . We then have  $\hat{\theta}_{n'_1+n'_2, \xi} = \bar{\theta} + (\|\bar{\theta}\|/(\bar{\rho}\sqrt{n'_1+n'_2}))z$  with  $\xi = 1$ .

It follows from applying Theorem 1 to the model trained on the combined data (Assumption 3) that the resulting linear trend achieves

$$\text{Slope}(\hat{\theta}_{n'_1+n'_2, \xi}(\mathcal{D}_{n'_1, \tilde{\theta}_1, \tilde{\rho}_1} \cup \mathcal{D}_{n'_2, \tilde{\theta}_2, \tilde{\rho}_2})) := \frac{\cos(\theta_2, \bar{\theta})\rho_2}{\cos(\theta_1, \bar{\theta})\rho_1}, \quad (3)$$

We show that the slope obtained from training on the combined dataset lies between those obtained from training on the two datasets separately. The proof could be found in Appendix F.2. Let  $\text{Slope}_1 := \text{Slope}(\hat{\theta}_{n_1}(\mathcal{D}_{n_1, \hat{\theta}_1, \hat{\rho}_1}))$  and  $\text{Slope}_2$  be defined similarly.

**Theorem 2.** *Under Assumption 3,  $\text{Slope}_1 \leq \text{Slope}(\hat{\theta}_{n'_1+n'_2}(\mathcal{D}_{n'_1, \hat{\theta}_1, \hat{\rho}_1} \cup \mathcal{D}_{n'_2, \hat{\theta}_2, \hat{\rho}_2})) \leq \text{Slope}_2$ .*

### 6.3 Filtering Data to Improve Robustness

The input mixing analysis in Section 6.2 suggests a filtering strategy to improve robustness.

**Assumption 4** (Gaussian distributions for filtering). *Consider a training dataset  $\mathcal{D}_{n, \theta_{\text{train}}, \rho}$  of size  $n$  draw i.i.d. from  $(X, Y) \sim P_{\theta_{\text{train}}, \rho}$  where  $Y = \pm 1$  uniformly at random and  $X|Y \sim \mathcal{N}(Y\theta_{\text{train}}, (\|\theta_{\text{train}}\|/\rho)^2 \mathbf{I})$ . A model trained on an unfiltered  $\mathcal{D}_{n, \theta_{\text{train}}, \rho}$  is denoted by  $\hat{\theta}_{\text{unfiltered}} = (1/n) \sum_{(x_i, y_i) \in \mathcal{D}_{n, \theta_{\text{train}}, \rho}} x_i y_i$ . Note that  $\hat{\theta}_{\text{unfiltered}} \sim \mathcal{N}(\theta_{\text{train}}, (\|\theta_{\text{train}}\|/(\rho\sqrt{n}))^2 \mathbf{I})$ .*

*The model is evaluated on two test datasets: in-distribution (ID) and out-of-distribution (OOD), each with an isotropic Gaussian noise:  $(X, Y) \sim P_{\theta_{\text{ID}}, \rho_{\text{ID}}}$ , where  $Y = \pm 1$  uniformly at random and  $X|Y \sim \mathcal{N}(Y\theta_{\text{ID}}, (\|\theta_{\text{ID}}\|/\rho_{\text{ID}})^2 \mathbf{I})$ , and  $P_{\theta_{\text{OOD}}, \rho_{\text{OOD}}}$  is defined similarly. Let  $\text{Slope}(\theta) := \frac{\cos(\theta_{\text{OOD}}, \theta) \rho_{\text{OOD}}}{\cos(\theta_{\text{ID}}, \theta) \rho_{\text{ID}}}$  and assume that all models achieve better ID accuracy than OOD accuracy, i.e.,  $\text{Slope}(\theta) < 1$ . A model is more robust if the slope is closer to one.*

Suppose we have access to a pre-trained model  $\hat{\theta}_{\text{pretrained}}$  that achieves better robustness than the model  $\hat{\theta}_{\text{unfiltered}}$  trained on the unfiltered data, i.e.,  $\text{Slope}(\hat{\theta}_{\text{unfiltered}}) < \text{Slope}(\hat{\theta}_{\text{pretrained}}) \leq 1$ . We want to use the pre-trained model to filter the data  $\mathcal{D}_{n, \theta_{\text{train}}, \rho}$  and achieve better robustness. We consider a generic family of filtering strategies that subsamples each data point  $(x_i, y_i) \in \mathcal{D}_{n, \theta_{\text{train}}, \rho}$  with probability that is monotonically non-decreasing with its correlation to the pre-trained model, i.e.,  $\mathbb{P}((x_i, y_i) \text{ passes the filter}) \propto h(\langle x_i y_i, \hat{\theta}_{\text{pretrained}} \rangle)$  for some monotonic scalar function  $h: \mathbb{R} \rightarrow \mathbb{R}_+$ . We analyze the model  $\hat{\theta}_{\text{filtered}} = (1/m) \sum_{(x_i, y_i) \in \text{filtered dataset}} x_i y_i$ . The next theorem shows that any such filtering strategy improves robustness, and the full proof can be found in Appendix F.3.

**Theorem 3.** *Under Assumption 4, if  $\text{Slope}(\hat{\theta}_{\text{unfiltered}}) < \text{Slope}(\hat{\theta}_{\text{pretrained}}) \leq 1$  then any model  $\hat{\theta}_{\text{filtered}}$  that is trained on the above family of filtered datasets achieves better robustness than the model trained on unfiltered data:  $\text{Slope}(\hat{\theta}_{\text{unfiltered}}) < \text{Slope}(\mathbb{E}[\hat{\theta}_{\text{filtered}}]) \leq \text{Slope}(\hat{\theta}_{\text{pretrained}})$ , where  $\text{Slope}(\mathbb{E}[\hat{\theta}_{\text{filtered}}])$  denotes the slope of the linear trend of a model trained on the filtered data.*

*Remark 3. Relevance to empirical practice:* The data filtering approach currently employed for the LAION dataset [68] motivates our theoretical setup. The authors of LAION first retrieved a large number of image-text pairs from Common Crawl [1] and then computed the cosine similarity between the image and text embeddings using one of the CLIP models originally introduced by Radford et al. [61]. Next, the authors removed all pairs with similarity less than 0.3 from the dataset. While it was initially unclear if filtering the noisy Common Crawl source with an existing CLIP model would lead to a dataset with good generalization properties, experiments with medium-scale models on LAION so far demonstrate that the resulting models are comparable to the original CLIP models [2].

Our theorem 3 does not provide a full justification for the filtering process described above, but it offers theoretical evidence that filtering a noisy data source with an existing robust model can indeed improve the effective robustness of the resulting dataset. It remains to be shown empirically that the slope of the linear trend exhibited by the CLIP model from [61] is larger than that of a

model trained on the Common Crawl data pool without filtering. If this assumption holds, we can expect that training on data with better text-image alignment according to the original CLIP model, will improve robustness compared to training on unfiltered data from Common Crawl.

## 7 Conclusion

Motivated by CLIP’s robustness to distribution shift, we introduced a testbed of six image-text datasets to study the influence of pre-training data on the robustness of multimodal models such as CLIP. We analyzed the interactions of these datasets through both experiments and theoretical analyses, finding that simply combining multiple datasets dilutes the robustness of the best-performing one. Moreover, we offer an explanation for the potential benefits of the data filtering process currently used for LAION. Our findings suggest that training on a carefully selected subset of data may provide more robustness than training on simply more data, for example, obtained by combining multiple data sources.

To summarize, our results lead to the following recommendations for dataset design:

- On the evaluation front: building a pre-training dataset requires multiple robustness test sets, as we have shown that different pre-training datasets exhibit substantially different behaviors across distribution shifts.
- On the dataset design front: each candidate data source for the overall pre-training dataset should be evaluated separately for its generalization and robustness properties. The final pre-training dataset should then contain more samples from the higher-quality pre-training sources. Creating a more “diverse” pre-training dataset by randomly sampling from all candidate sources does not result in a better dataset.
- Assuming access to models separately trained on each source of interest, output ensemble is a good predictor of the effective robustness obtained from input mixing, and hence can significantly reduce the time to search for the right mixing strategy.
- Filtering a noisy data source with an existing robust model can improve the generalization properties of the resulting dataset.

The broad societal implications of image-text models and web-crawled multimodal datasets have been extensively discussed by Radford et al. [61] and Birhane et al. [10] respectively. As these models continue to grow in size, full-scale experiments are becoming prohibitively expensive. This necessitates small, systematic experiments that allow reliable extrapolation to larger scales. Since effective robustness is independent of model size and quantity of training data, we hope that our testbed and results can serve as a first step towards building multimodal pre-training datasets in a principled manner.

### 7.1 Limitations

The pre-training datasets we experiment with range from 5M to 15M samples. While this lags behind current state-of-the-art settings that large image-text models are often trained on, we believe our findings also hold for models with higher accuracy for the following reasons:

- The original CLIP paper [61] offers evidence showing that CLIP’s performance exhibits reliable linear trends across compute scales (Figure 9 of [61], which includes the ResNet50-encoder that our paper works with) and performance on natural distribution shifts (Figure 14 of [61]). In particular, the linear trends in this Figure 14 are analogous to the linear trends in our scatter plots.
- In the OpenCLIP GitHub repository [38] that seeks to match the performance of the original CLIP paper, the authors there also note that their models that were trained on 15M samples or fewer share the same effective robustness trend as OpenAI’s CLIP models (trained on 400M samples). Refer to their [Why are low-accuracy CLIP models interesting?](#) remark for more details.
- Previous work [52] has experimented with training on randomly sampled subsets of the training dataset to produce models covering a wide range of accuracies, and found that these models lie on the same effective robustness trend. This includes models trained on only 1% of the original data, which matches the scale of our experiments (5M-15M samples) relative to the scale of the original CLIP paper (400M samples).

The focus of our work is to study the behavior of a diverse set of data sources, and performing full-scale experiments on 6 datasets (and their combinations) would be prohibitively expensive. To provide some perspectives on the amount of resources involved in full-scale experiments: (i) One of the larger datasets that are publicly available, LAION-5B, is a substantial effort that involves 14 people actively working on it [2], (ii) Training a ResNet50-encoder CLIP on the full dataset of 400M samples took 18 days on 592 V100 GPUs, according to the original paper [61]. This prompts us to leverage publicly available web-crawled datasets, and study the behavior of our trained models through the effective robustness framework, which has been shown to be scale-invariant.

## 7.2 Future Research Directions

Our findings motivate a number of interesting future directions, which we summarize below:

### Data sources

- *Comparing more data sources:* Our testbed of six image-text datasets is only a first step toward mapping the landscape of pre-training datasets for vision-language models. There are many more web sources from which pre-training datasets could be assembled for interesting comparisons, e.g., web searches, further social media sites (Pinterest, Tumblr, etc.), or captioned videos from YouTube, to name a few. In addition, there are also more domain-specific data sources such as iNaturalist [79], BigEarthNet [73], and Patch Camelyon [80] that likely offer complementary robustness profiles. An interesting outcome of this research direction would be a “dataset atlas” that allows practitioners to quickly identify relevant pre-training datasets for their task of interest.
- *Synthetic pre-training data:* The datasets in our testbed contain images and text initially created by humans for other purposes and then assembled into a dataset for model training. An interesting alternative is to create training data specifically to improve the generalization of image-text models. There are at least three potential avenues: (i) Rendering virtual 3D environments [27, 30, 50], (ii) text-to-image generative models [55, 64, 67, 85], and (iii) image captioning models [53, 72, 89]. All three avenues offer more fine-grained control over the training data, but in all three cases it is not yet well understood how synthetic data affects robustness.



- *Data efficiency*: Our focus has been on the impact of datasets on generalization through the lens of effective robustness, which depends only on the training *distribution*, not the number of samples drawn from the distribution [52]. A natural complementary question is how the datasets in our testbed compare in terms of their scaling behavior with training set size. For instance, it may be the case that some datasets offer less effective robustness, but the absolute accuracy numbers may improve more quickly with increasing dataset size than for other data sources.

This direction is closely related to empirical scaling laws for neural networks [12, 23, 40, 59], which have recently gained attention because the laws aim to predict model performance as model size, compute, or amount of training data increases. We provide initial experiments on data scaling for our testbed with minimal hyperparameter tuning in Appendix C (Figure 17). Understanding these trends in more detail and testing their reliability (e.g., under hyperparameter variations) may serve as a starting point for future work.

## Understanding and improving dataset curation

- *Combining data sources at a more fine-grained level*: We have shown both empirically and in our theoretical model that simply taking the union of two datasets dilutes the robustness of the better dataset. This suggests that improving robust generalization may require more sophisticated methods to combine datasets, e.g., by selecting individual samples or subsets from each dataset with complementary generalization properties. We posit that this approach could take inspiration from the subset selection literature [18, 41, 57, 70].
- *Data filtering techniques*: Some of the datasets in our testbed such as LAION and YFCC-15M do not contain “raw” unfiltered data from the web. Instead, they are already the result of an initial filtering process. In both cases, this filtering process reduces the size of the dataset by a factor of seven to eight, and the impact of this filtering on generalization is currently not well understood. In addition, the filtering approaches can vary substantially: OpenAI built YFCC-15M from hand-crafted rules while LAION relied on CLIP models for their filtering process. Experimentally exploring the effect of these filtering processes is likely an important direction for future work since the filtering step removes a large number of potential training examples. Two concrete questions would be whether using higher-accuracy models in the context of LAION’s filtering process leads to better datasets, and comparing the LAION dataset to an unfiltered sample from the same source (Common Crawl).

## Theory

- *More general theoretical models*: Our theoretical model could be extended so it is more aligned with standard experimental settings, e.g., by increasing the number of classes beyond two, or by including more complex classifiers beyond the linear model we currently examine. Furthermore, Miller et al. [52] have shown that non-isotropic covariance shifts in the data distribution lead to a deviation from the linear trend, at least for fixed classifiers independent of the training data. In future work, we would like to develop similar theoretical analyses involving covariance shifts, but for classifiers with explicit dependence on the training distribution and training set size, similar to what we have studied in this paper.
- *Low-accuracy regime*: The emergence of linear trends relating in-distribution to out-of-distribution accuracy in our theoretical models is consistent with our empirical observations for classifiers

that reach at least 10% accuracy on ImageNet. On the other hand, in a lower accuracy regime, our theoretical analyses predict that any trained model approaches the in-distribution and out-of-distribution accuracy of random guessing (see Remark 2 in Section 6.1). Future work should empirically explore models with lower zero-shot accuracies (e.g., by reducing the pre-training dataset size) to see how the empirical trends behave in a lower accuracy regime. If the intercept is not at the accuracy of random guessing, this suggests an area of improvement for the theoretical analysis to better fit these new empirical observations in the low-accuracy regime.

## Further directions

- *Connections to large language models:* Our focus in this paper has been on vision-language models. Another area where large pre-training sets are essential is unimodal language models [12, 21, 37, 47, 62, 77]. Many of the questions we address in this paper also arise in the context of language models. A first step in this direction would be to assemble a comprehensive robustness testbed for NLP tasks to measure the extent to which the “accuracy on the line” phenomenon uncovered by Miller et al. [52] also holds in NLP. One recent set of experiments indicates that this may be the case [51], but they do not yet include recent large language models such as GPT-3 [12].
- *Dataset design for fine-tuning:* We have studied the robustness properties of *zero-shot* models, but the models can often also be fine-tuned on task-specific data to increase performance on a target task. It remains an open question how the pre-training dataset affects the generalization properties of models after an extra fine-tuning step.

We look forward to addressing these topics in our future work.

## Acknowledgements

We would like to thank Tiffany Cai, Nicholas Carlini, Tatsunori Hashimoto, Jong Wook Kim, Hongseok Namkoong, Alec Radford, Rohan Taori, and Thomas Wolf for helpful discussions while working on this paper. We also thank Tiffany Cai and Jack Gallagher for their help with the dataset collection. HuggingFace has provided generous assistance in the form of compute resources that made many of our experiments possible. In particular, we would like to thank Leandro von Werra and Victor Sanh for their help with setting up the compute infrastructure and their constructive feedback on the dataset testbed. This work is supported in part by Open Philanthropy, the Allen Institute for AI, and NSF grants CNS-2002664, IIS-1929955, DMS-2134012, and CCF-2019844 as a part of NSF Institute for Foundations of Machine Learning (IFML).

## References

- [1] Common crawl. <https://commoncrawl.org/>. Accessed: 2022-05-18.
- [2] Laion-5b: A new era of open large-scale multi-modal datasets. <https://laion.ai/laion-5b-a-new-era-of-open-large-scale-multi-modal-datasets/>. Accessed: 2022-05-18.
- [3] Jean-Baptiste Alayrac, Jeff Donahue, Pauline Luc, Antoine Miech, Iain Barr, Yana Hasson, Karel Lenc, Arthur Mensch, Katie Millican, Malcolm Reynolds, et al. Flamingo: a visual language model for few-shot learning. *arXiv preprint arXiv:2204.14198*, 2022.

- [4] Anders Andreassen, Yasaman Bahri, Behnam Neyshabur, and Rebecca Roelofs. The evolution of out-of-distribution robustness throughout fine-tuning, 2021. <https://arxiv.org/abs/2106.15831>.
- [5] Martin Arjovsky, Léon Bottou, Ishaan Gulrajani, and David Lopez-Paz. Invariant risk minimization, 2019. <https://arxiv.org/abs/1907.02893>.
- [6] Andrei Barbu, David Mayo, Julian Alverio, William Luo, Christopher Wang, Dan Gutfreund, Josh Tenenbaum, and Boris Katz. Objectnet: A large-scale bias-controlled dataset for pushing the limits of object recognition models. *Advances in neural information processing systems*, 32, 2019.
- [7] Eric Bauer and Ron Kohavi. An empirical comparison of voting classification algorithms: Bagging, boosting, and variants. *Machine learning*, 1999. <https://link.springer.com/article/10.1023/A:1007515423169>.
- [8] Battista Biggio and Fabio Roli. Wild patterns: Ten years after the rise of adversarial machine learning. *Pattern Recognition*, 84:317–331, 2018.
- [9] Battista Biggio, Iginio Corona, Davide Maiorca, Blaine Nelson, Nedim Šrđić, Pavel Laskov, Giorgio Giacinto, and Fabio Roli. Evasion attacks against machine learning at test time. In *Joint European conference on machine learning and knowledge discovery in databases*, pages 387–402. Springer, 2013.
- [10] Abeba Birhane, Vinay Uday Prabhu, and Emmanuel Kahembwe. Multimodal datasets: misogyny, pornography, and malignant stereotypes. *arXiv preprint arXiv:2110.01963*, 2021.
- [11] Leo Breiman. Bagging predictors. *Machine learning*, 1996. <https://link.springer.com/article/10.1007/BF00058655>.
- [12] Tom Brown, Benjamin Mann, Nick Ryder, Melanie Subbiah, Jared D Kaplan, Prafulla Dhariwal, Arvind Neelakantan, Pranav Shyam, Girish Sastry, Amanda Askell, et al. Language models are few-shot learners. *Advances in neural information processing systems*, 33:1877–1901, 2020.
- [13] Soravit Changpinyo, Piyush Sharma, Nan Ding, and Radu Soricut. Conceptual 12m: Pushing web-scale image-text pre-training to recognize long-tail visual concepts. In *Proceedings of the IEEE/CVF Conference on Computer Vision and Pattern Recognition*, pages 3558–3568, 2021.
- [14] Ting Chen, Simon Kornblith, Mohammad Norouzi, and Geoffrey Hinton. A simple framework for contrastive learning of visual representations. In *International conference on machine learning*, pages 1597–1607. PMLR, 2020.
- [15] Aakanksha Chowdhery, Sharan Narang, Jacob Devlin, Maarten Bosma, Gaurav Mishra, Adam Roberts, Paul Barham, Hyung Won Chung, Charles Sutton, Sebastian Gehrmann, et al. Palm: Scaling language modeling with pathways. *arXiv preprint arXiv:2204.02311*, 2022.
- [16] Alexander D’Amour, Katherine Heller, Dan Moldovan, Ben Adlam, Babak Alipanahi, Alex Beutel, Christina Chen, Jonathan Deaton, Jacob Eisenstein, Matthew D Hoffman, et al. Underspecification presents challenges for credibility in modern machine learning, 2020. <https://arxiv.org/abs/2011.03395>.

- [17] Luke N Darlow, Elliot J Crowley, Antreas Antoniou, and Amos J Storkey. Cinic-10 is not imagenet or cifar-10. *arXiv preprint arXiv:1810.03505*, 2018.
- [18] Sanjoy Dasgupta, Daniel Hsu, Stefanos Poulis, and Xiaojin Zhu. Teaching a black-box learner. In *International Conference on Machine Learning*, pages 1547–1555. PMLR, 2019.
- [19] Jia Deng, Wei Dong, Richard Socher, Li-Jia Li, Kai Li, and Li Fei-Fei. Imagenet: A large-scale hierarchical image database. In *Conference on Computer Vision and Pattern Recognition*, 2009. <https://ieeexplore.ieee.org/document/5206848>.
- [20] Karan Desai, Gaurav Kaul, Zubin Aysola, and Justin Johnson. Redcaps: Web-curated image-text data created by the people, for the people. *arXiv preprint arXiv:2111.11431*, 2021.
- [21] Jacob Devlin, Ming-Wei Chang, Kenton Lee, and Kristina Toutanova. Bert: Pre-training of deep bidirectional transformers for language understanding. *arXiv preprint arXiv:1810.04805*, 2018.
- [22] Thomas G Dietterich. Ensemble methods in machine learning. In *International workshop on multiple classifier systems*, 2000. [https://link.springer.com/chapter/10.1007/3-540-45014-9\\_1](https://link.springer.com/chapter/10.1007/3-540-45014-9_1).
- [23] Josip Djolonga, Jessica Yung, Michael Tschannen, Rob Romijnders, Lucas Beyer, Alexander Kolesnikov, Joan Puigcerver, Matthias Minderer, Alexander D’Amour, Dan Moldovan, et al. On robustness and transferability of convolutional neural networks. In *Proceedings of the IEEE/CVF Conference on Computer Vision and Pattern Recognition*, pages 16458–16468, 2021.
- [24] Alex Fang, Gabriel Ilharco, Mitchell Wortsman, Yuhao Wan, Vaishaal Shankar, Achal Dave, and Ludwig Schmidt. Data determines distributional robustness in contrastive language image pre-training (clip). *arXiv preprint arXiv:2205.01397*, 2022.
- [25] Stanislav Fort, Huiyi Hu, and Balaji Lakshminarayanan. Deep ensembles: A loss landscape perspective, 2019. <https://arxiv.org/abs/1912.02757>.
- [26] Yoav Freund and Robert E Schapire. A decision-theoretic generalization of on-line learning and an application to boosting. *Journal of Computer and System Sciences*, 1997. <https://www.sciencedirect.com/science/article/pii/S002200009791504X>.
- [27] Huan Fu, Rongfei Jia, Lin Gao, Mingming Gong, Binqiang Zhao, Steve Maybank, and Dacheng Tao. 3d-future: 3d furniture shape with texture. *International Journal of Computer Vision*, pages 1–25, 2021.
- [28] Peng Gao, Shijie Geng, Renrui Zhang, Teli Ma, Rongyao Fang, Yongfeng Zhang, Hongsheng Li, and Yu Qiao. Clip-adapter: Better vision-language models with feature adapters, 2021. <https://arxiv.org/abs/2110.04544>.
- [29] Raphael Gontijo-Lopes, Yann Dauphin, and Ekin D Cubuk. No one representation to rule them all: Overlapping features of training methods, 2021. <https://arxiv.org/abs/2007.01434>.
- [30] Klaus Greff, Francois Belletti, Lucas Beyer, Carl Doersch, Yilun Du, Daniel Duckworth, David J Fleet, Dan Gnanapragasam, Florian Golemo, Charles Herrmann, et al. Kubric: A scalable dataset generator. In *Proceedings of the IEEE/CVF Conference on Computer Vision and Pattern Recognition*, pages 3749–3761, 2022.

- [31] Ishaan Gulrajani and David Lopez-Paz. In search of lost domain generalization. *International Conference on Learning Representations (ICLR)*, 2020. <https://arxiv.org/abs/2007.01434>.
- [32] Kaiming He, Xiangyu Zhang, Shaoqing Ren, and Jian Sun. Deep residual learning for image recognition. In *Proceedings of the IEEE conference on computer vision and pattern recognition*, pages 770–778, 2016.
- [33] Kaiming He, Haoqi Fan, Yuxin Wu, Saining Xie, and Ross Girshick. Momentum contrast for unsupervised visual representation learning. In *Proceedings of the IEEE/CVF conference on computer vision and pattern recognition*, pages 9729–9738, 2020.
- [34] Kaiming He, Xinlei Chen, Saining Xie, Yanghao Li, Piotr Dollár, and Ross Girshick. Masked autoencoders are scalable vision learners. In *Proceedings of the IEEE/CVF Conference on Computer Vision and Pattern Recognition*, pages 16000–16009, 2022.
- [35] Dan Hendrycks and Thomas Dietterich. Benchmarking neural network robustness to common corruptions and perturbations. *International Conference on Learning Representations (ICLR)*, 2019. <https://arxiv.org/abs/1903.12261>.
- [36] Dan Hendrycks, Steven Basart, Norman Mu, Saurav Kadavath, Frank Wang, Evan Dorundo, Rahul Desai, Tyler Zhu, Samyak Parajuli, Mike Guo, et al. The many faces of robustness: A critical analysis of out-of-distribution generalization. In *Proceedings of the IEEE/CVF International Conference on Computer Vision*, pages 8340–8349, 2021.
- [37] Jordan Hoffmann, Sebastian Borgeaud, Arthur Mensch, Elena Buchatskaya, Trevor Cai, Eliza Rutherford, Diego de Las Casas, Lisa Anne Hendricks, Johannes Welbl, Aidan Clark, et al. Training compute-optimal large language models. *arXiv preprint arXiv:2203.15556*, 2022.
- [38] Gabriel Ilharco, Mitchell Wortsman, Nicholas Carlini, Rohan Taori, Achal Dave, Vaishaal Shankar, Hongseok Namkoong, John Miller, Hannaneh Hajishirzi, Ali Farhadi, and Ludwig Schmidt. Openclip, July 2021. URL <https://doi.org/10.5281/zenodo.5143773>. If you use this software, please cite it as below.
- [39] Chao Jia, Yinfei Yang, Ye Xia, Yi-Ting Chen, Zarana Parekh, Hieu Pham, Quoc Le, Yun-Hsuan Sung, Zhen Li, and Tom Duerig. Scaling up visual and vision-language representation learning with noisy text supervision. In *International Conference on Machine Learning*, pages 4904–4916. PMLR, 2021.
- [40] Jared Kaplan, Sam McCandlish, Tom Henighan, Tom B Brown, Benjamin Chess, Rewon Child, Scott Gray, Alec Radford, Jeffrey Wu, and Dario Amodei. Scaling laws for neural language models. *arXiv preprint arXiv:2001.08361*, 2020.
- [41] Krishnateja Killamsetty, S Durga, Ganesh Ramakrishnan, Abir De, and Rishabh Iyer. Grad-match: Gradient matching based data subset selection for efficient deep model training. In *International Conference on Machine Learning*, pages 5464–5474. PMLR, 2021.
- [42] Pang Wei Koh, Shiori Sagawa, Henrik Marklund, Sang Michael Xie, Marvin Zhang, Akshay Balsubramani, Weihua Hu, Michihiro Yasunaga, Richard Lanus Phillips, Irena Gao, et al. Wilds: A benchmark of in-the-wild distribution shifts. In *International Conference on Machine Learning*, pages 5637–5664. PMLR, 2021.

- [43] Alex Krizhevsky, Geoffrey Hinton, et al. Learning multiple layers of features from tiny images. 2009.
- [44] David Krueger, Ethan Caballero, Joern-Henrik Jacobsen, Amy Zhang, Jonathan Binas, Dinghui Zhang, Remi Le Priol, and Aaron Courville. Out-of-distribution generalization via risk extrapolation (rex), 2021. <https://arxiv.org/abs/2003.00688>.
- [45] Balaji Lakshminarayanan, Alexander Pritzel, and Charles Blundell. Simple and scalable predictive uncertainty estimation using deep ensembles. In *Advances in Neural Information Processing Systems (NeurIPS)*, 2017. <https://arxiv.org/abs/1612.01474>.
- [46] Yangguang Li, Feng Liang, Lichen Zhao, Yufeng Cui, Wanli Ouyang, Jing Shao, Fengwei Yu, and Junjie Yan. Supervision exists everywhere: A data efficient contrastive language-image pre-training paradigm. *arXiv preprint arXiv:2110.05208*, 2021.
- [47] Opher Lieber, Or Sharir, Barak Lenz, and Yoav Shoham. Jurassic-1: Technical details and evaluation. *White Paper. AI21 Labs*, 2021.
- [48] Ilya Loshchilov and Frank Hutter. Sgdr: Stochastic gradient descent with warm restarts. *arXiv preprint arXiv:1608.03983*, 2016.
- [49] Ilya Loshchilov and Frank Hutter. Decoupled weight decay regularization. *arXiv preprint arXiv:1711.05101*, 2017.
- [50] John McCormac, Ankur Handa, Stefan Leutenegger, and Andrew J Davison. Scenenet rgb-d: 5m photorealistic images of synthetic indoor trajectories with ground truth. *arXiv preprint arXiv:1612.05079*, 2016.
- [51] John Miller, Karl Krauth, Benjamin Recht, and Ludwig Schmidt. The effect of natural distribution shift on question answering models. In *International Conference on Machine Learning*, pages 6905–6916. PMLR, 2020.
- [52] John P Miller, Rohan Taori, Aditi Raghunathan, Shiori Sagawa, Pang Wei Koh, Vaishaal Shankar, Percy Liang, Yair Carmon, and Ludwig Schmidt. Accuracy on the line: on the strong correlation between out-of-distribution and in-distribution generalization. In *International Conference on Machine Learning*, pages 7721–7735. PMLR, 2021.
- [53] Ron Mokady, Amir Hertz, and Amit H Bermano. Clipcap: Clip prefix for image captioning. *arXiv preprint arXiv:2111.09734*, 2021.
- [54] Norman Mu, Alexander Kirillov, David Wagner, and Saining Xie. Slip: Self-supervision meets language-image pre-training. *arXiv preprint arXiv:2112.12750*, 2021.
- [55] Alex Nichol, Prafulla Dhariwal, Aditya Ramesh, Pranav Shyam, Pamela Mishkin, Bob McGrew, Ilya Sutskever, and Mark Chen. Glide: Towards photorealistic image generation and editing with text-guided diffusion models. *arXiv preprint arXiv:2112.10741*, 2021.
- [56] Jeremy Nixon, Balaji Lakshminarayanan, and Dustin Tran. Why are bootstrapped deep ensembles not better? In *"I Can't Believe It's Not Better!" NeurIPS 2020 workshop*, 2020. URL <https://openreview.net/forum?id=dTCir0ceyv0>.



- [57] Mansheej Paul, Surya Ganguli, and Gintare Karolina Dziugaite. Deep learning on a data diet: Finding important examples early in training. *Advances in Neural Information Processing Systems*, 34:20596–20607, 2021.
- [58] Hieu Pham, Zihang Dai, Golnaz Ghiasi, Hanxiao Liu, Adams Wei Yu, Minh-Thang Luong, Mingxing Tan, and Quoc V Le. Combined scaling for zero-shot transfer learning. *arXiv preprint arXiv:2111.10050*, 2021.
- [59] Gabriele Prato, Simon Guiroy, Ethan Caballero, Irina Rish, and Sarath Chandar. Scaling laws for the few-shot adaptation of pre-trained image classifiers. *arXiv preprint arXiv:2110.06990*, 2021.
- [60] Joaquin Quiñonero-Candela, Masashi Sugiyama, Anton Schwaighofer, and Neil D Lawrence. *Dataset shift in machine learning*. Mit Press, 2008.
- [61] Alec Radford, Jong Wook Kim, Chris Hallacy, Aditya Ramesh, Gabriel Goh, Sandhini Agarwal, Girish Sastry, Amanda Askell, Pamela Mishkin, Jack Clark, et al. Learning transferable visual models from natural language supervision. In *International Conference on Machine Learning*, pages 8748–8763. PMLR, 2021.
- [62] Jack W Rae, Sebastian Borgeaud, Trevor Cai, Katie Millican, Jordan Hoffmann, Francis Song, John Aslanides, Sarah Henderson, Roman Ring, Susannah Young, et al. Scaling language models: Methods, analysis & insights from training gopher. *arXiv preprint arXiv:2112.11446*, 2021.
- [63] Aditya Ramesh, Mikhail Pavlov, Gabriel Goh, Scott Gray, Chelsea Voss, Alec Radford, Mark Chen, and Ilya Sutskever. Zero-shot text-to-image generation. In *International Conference on Machine Learning*, pages 8821–8831. PMLR, 2021.
- [64] Aditya Ramesh, Prafulla Dhariwal, Alex Nichol, Casey Chu, and Mark Chen. Hierarchical text-conditional image generation with clip latents. *arXiv preprint arXiv:2204.06125*, 2022.
- [65] Benjamin Recht, Rebecca Roelofs, Ludwig Schmidt, and Vaishaal Shankar. Do imagenet classifiers generalize to imagenet? In *International Conference on Machine Learning*, pages 5389–5400. PMLR, 2019.
- [66] Shiori Sagawa, Pang Wei Koh, Tatsunori B Hashimoto, and Percy Liang. Distributionally robust neural networks for group shifts: On the importance of regularization for worst-case generalization, 2019. <https://arxiv.org/abs/1911.08731>.
- [67] Chitwan Saharia, William Chan, Saurabh Saxena, Lala Li, Jay Whang, Emily Denton, Seyed Kamyar Seyed Ghasemipour, Burcu Karagol Ayan, S Sara Mahdavi, Rapha Gontijo Lopes, et al. Photorealistic text-to-image diffusion models with deep language understanding. *arXiv preprint arXiv:2205.11487*, 2022.
- [68] Christoph Schuhmann, Richard Vencu, Romain Beaumont, Robert Kaczmarczyk, Clayton Mullis, Aarush Katta, Theo Coombes, Jenia Jitsev, and Aran Komatsuzaki. Laion-400m: Open dataset of clip-filtered 400 million image-text pairs. *arXiv preprint arXiv:2111.02114*, 2021.
- [69] Vaishaal Shankar, Rebecca Roelofs, Horia Mania, Alex Fang, Benjamin Recht, and Ludwig Schmidt. Evaluating machine accuracy on imagenet. In *International Conference*

- on Machine Learning (ICML), 2020. <http://proceedings.mlr.press/v119/shankar20c/shankar20c.pdf>.
- [70] Ben Sorscher, Robert Geirhos, Shashank Shekhar, Surya Ganguli, and Ari S Morcos. Beyond neural scaling laws: beating power law scaling via data pruning. *arXiv preprint arXiv:2206.14486*, 2022.
  - [71] Krishna Srinivasan, Karthik Raman, Jiecao Chen, Michael Bendersky, and Marc Najork. Wit: Wikipedia-based image text dataset for multimodal multilingual machine learning. In *Proceedings of the 44th International ACM SIGIR Conference on Research and Development in Information Retrieval*, pages 2443–2449, 2021.
  - [72] Matteo Stefanini, Marcella Cornia, Lorenzo Baraldi, Silvia Cascianelli, Giuseppe Fiameni, and Rita Cucchiara. From show to tell: A survey on image captioning. *arXiv preprint arXiv:2107.06912*, 2021.
  - [73] Gencer Sumbul, Marcela Charfuelan, Beg"um Demir, and Volker Markl. Bigearthnet: A large-scale benchmark archive for remote sensing image understanding. *CoRR*, abs/1902.06148, 2019.
  - [74] Christian Szegedy, Wojciech Zaremba, Ilya Sutskever, Joan Bruna, Dumitru Erhan, Ian Goodfellow, and Rob Fergus. Intriguing properties of neural networks. *arXiv preprint arXiv:1312.6199*, 2013.
  - [75] Rohan Taori, Achal Dave, Vaishaal Shankar, Nicholas Carlini, Benjamin Recht, and Ludwig Schmidt. Measuring robustness to natural distribution shifts in image classification. *Advances in Neural Information Processing Systems*, 33:18583–18599, 2020.
  - [76] Bart Thomee, David A Shamma, Gerald Friedland, Benjamin Elizalde, Karl Ni, Douglas Poland, Damian Borth, and Li-Jia Li. Yfcc100m: The new data in multimedia research. *Communications of the ACM*, 59(2):64–73, 2016.
  - [77] Romal Thoppilan, Daniel De Freitas, Jamie Hall, Noam Shazeer, Apoorv Kulshreshtha, Heng-Tze Cheng, Alicia Jin, Taylor Bos, Leslie Baker, Yu Du, et al. Lamda: Language models for dialog applications. *arXiv preprint arXiv:2201.08239*, 2022.
  - [78] Antonio Torralba and Alexei A Efros. Unbiased look at dataset bias. In *CVPR 2011*, pages 1521–1528. IEEE, 2011.
  - [79] Grant Van Horn, Oisin Mac Aodha, Yang Song, Yin Cui, Chen Sun, Alex Shepard, Hartwig Adam, Pietro Perona, and Serge Belongie. The inaturalist species classification and detection dataset. In *Proceedings of the IEEE conference on computer vision and pattern recognition*, pages 8769–8778, 2018.
  - [80] Bastiaan S Veeling, Jasper Linmans, Jim Winkens, Taco Cohen, and Max Welling. Rotation equivariant cnns for digital pathology. In *International Conference on Medical image computing and computer-assisted intervention*, pages 210–218. Springer, 2018.
  - [81] Haohan Wang, Songwei Ge, Zachary Lipton, and Eric P Xing. Learning robust global representations by penalizing local predictive power. *Advances in Neural Information Processing Systems*, 32, 2019.

- [82] Mitchell Wortsman, Gabriel Ilharco, Jong Wook Kim, Mike Li, Simon Kornblith, Rebecca Roelofs, Raphael Gontijo-Lopes, Hannaneh Hajishirzi, Ali Farhadi, Hongseok Namkoong, and Ludwig Schmidt. Robust fine-tuning of zero-shot models. *arXiv preprint arXiv:2109.01903*, 2021. <https://arxiv.org/abs/2109.01903>.
- [83] Mitchell Wortsman, Gabriel Ilharco, Samir Yitzhak Gadre, Rebecca Roelofs, Raphael Gontijo-Lopes, Ari S Morcos, Hongseok Namkoong, Ali Farhadi, Yair Carmon, Simon Kornblith, et al. Model soups: averaging weights of multiple fine-tuned models improves accuracy without increasing inference time. *International Conference on Machine Learning (ICML)*, 2022. <https://arxiv.org/abs/2203.05482>.
- [84] Lewei Yao, Runhui Huang, Lu Hou, Guansong Lu, Minzhe Niu, Hang Xu, Xiaodan Liang, Zhenguo Li, Xin Jiang, and Chunjing Xu. Filip: Fine-grained interactive language-image pre-training. *arXiv preprint arXiv:2111.07783*, 2021.
- [85] Jiahui Yu, Yuanzhong Xu, Jing Yu Koh, Thang Luong, Gunjan Baid, Zirui Wang, Vijay Vasudevan, Alexander Ku, Yinfei Yang, Burcu Karagol Ayan, et al. Scaling autoregressive models for content-rich text-to-image generation. *arXiv preprint arXiv:2206.10789*, 2022.
- [86] Lu Yuan, Dongdong Chen, Yi-Ling Chen, Noel Codella, Xiyang Dai, Jianfeng Gao, Houdong Hu, Xuedong Huang, Boxin Li, Chunyuan Li, et al. Florence: A new foundation model for computer vision. *arXiv preprint arXiv:2111.11432*, 2021.
- [87] Renrui Zhang, Rongyao Fang, Peng Gao, Wei Zhang, Kunchang Li, Jifeng Dai, Yu Qiao, and Hongsheng Li. Tip-adapter: Training-free clip-adapter for better vision-language modeling, 2021. <https://arxiv.org/abs/2111.03930>.
- [88] Kaiyang Zhou, Jingkang Yang, Chen Change Loy, and Ziwei Liu. Conditional prompt learning for vision-language models. *Conference on Computer Vision and Pattern Recognition (CVPR)*, 2022. <https://arxiv.org/abs/2109.01134>.
- [89] Luowei Zhou, Hamid Palangi, Lei Zhang, Houdong Hu, Jason Corso, and Jianfeng Gao. Unified vision-language pre-training for image captioning and vqa. In *Proceedings of the AAAI Conference on Artificial Intelligence*, volume 34, pages 13041–13049, 2020.

## A Dataset Details

### A.1 Pre-training Datasets

Dataset	Source	Total Size
YFCC	Flickr	14,826,000
LAION	Common Crawl	15,504,742
CC-12M	Unspecified web pages	9,594,338
RedCaps	Reddit	11,882,403
WIT	Wikipedia	5,038,295
Shutterstock	Shutterstock	15,540,452

Table 1: Origin and total number of samples for each of the datasets we used in our experiments.

To get a better understanding of the diversity of different data sources, we analyze the distributions of caption lengths, image sizes and image aspect ratios for a set of 10,000 samples randomly selected from each source:

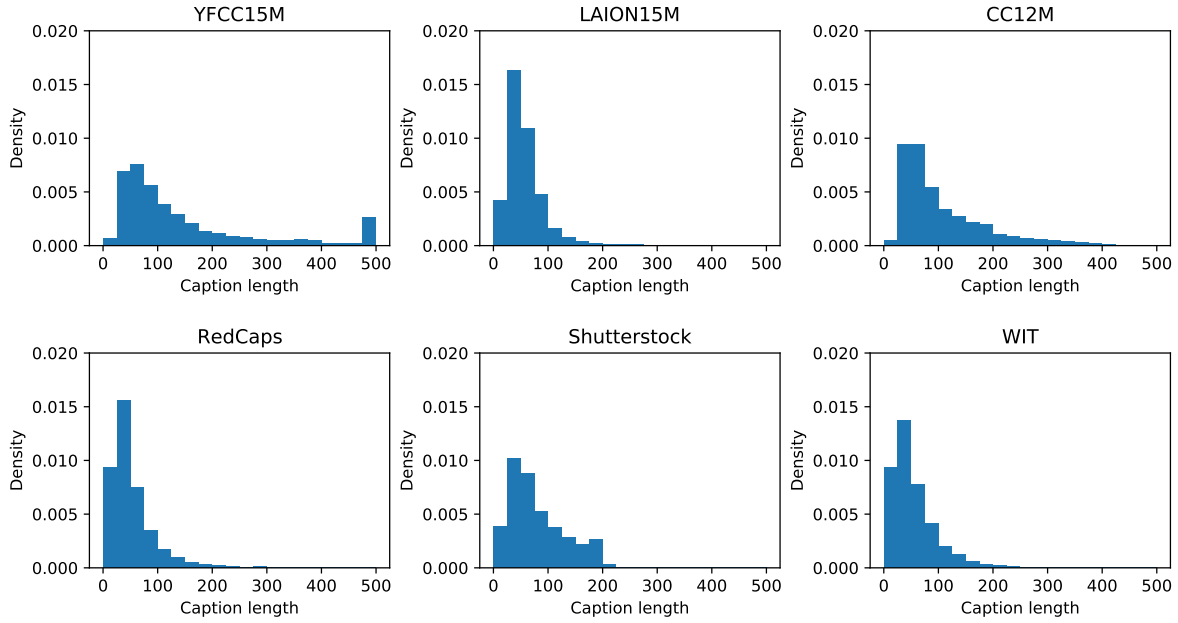


Figure 7: Distributions of caption lengths for each data source.

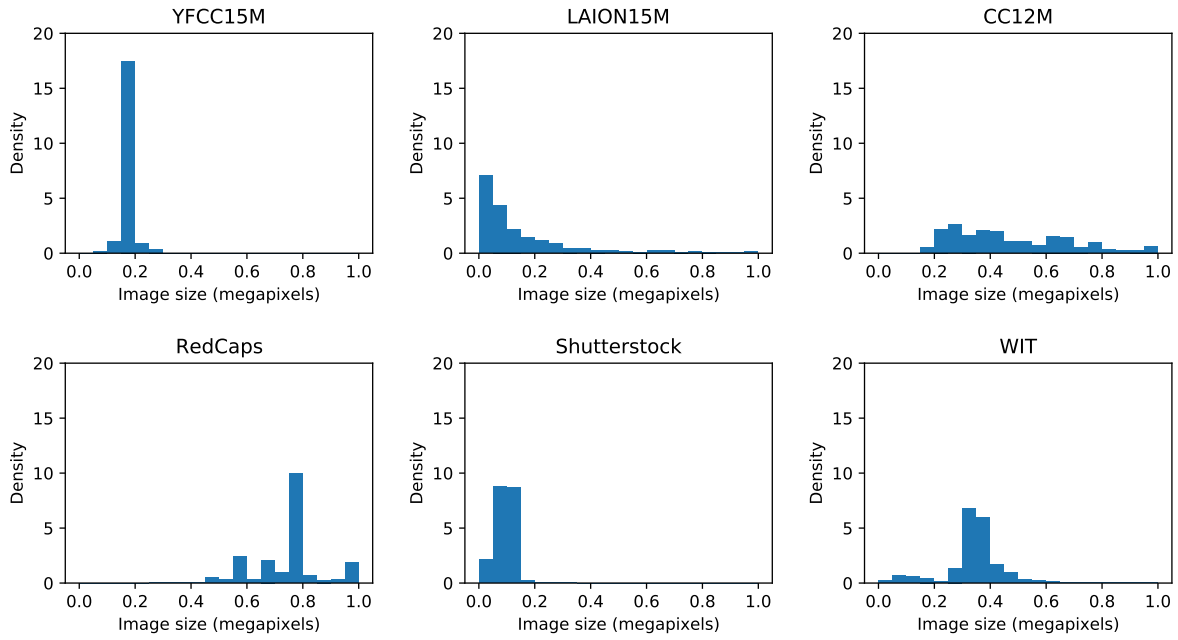


Figure 8: Distributions of image sizes for each data source.

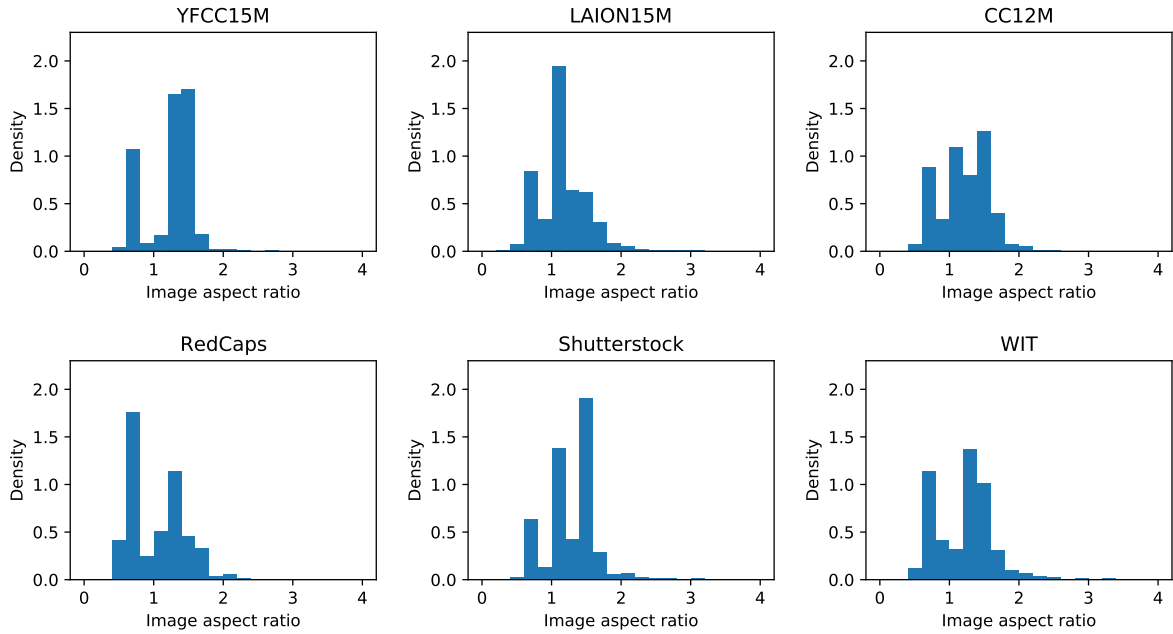


Figure 9: Distributions of image aspect ratios for each data source.

Below we also show some examples of image-caption pairs randomly selected from each data source:



Cody This picture is #5 in my 100 strangers project. Find out more about the project and see pictures taken by other photographers at [www.100Strangers.com](http://www.100Strangers.com).



Dan with the Man-Purse Dan Budiak, metrosexual



Cuffless To link or not to link, that is the question...



Dixie Union Chapel, 1836 Replaced a wooden structure that was built in 1816



ATWS Slide presentation from Sandra Carvao WTO\_0288 Slide presentation from Sandra Carvão Deputy Chief Market Intelligence and Promotion Department, World Tourism...



Web 2.0 Expo 2010 - San Francisco Please feel free to use this picture in your blog, website or presentation, in accordance with the stated Creative Commons and c...



Look out, King Vidor Jesse behind the lens. Jodhpurs and bullhorn not included.



Liverpool, England, United Kingdom Albert Dock - Liverpool, England, United Kingdom



Mariposa Butterfly



THATCamp Computational Archaeology August 2012, University of Virginia



Harry Potter and the Half Blood Prince Release Party / September 16 They had to release this thing on my anniversary? Follow the flag to get your book. Auntie's ...



Nicholas Yeager Co. C, 1st Arkansas Infantry



John Paul the Great St Patrick's Cathedral Charlotte NC May 20, 2007. We were there for the 33rd Annual Rosary Rally.



100 words for snow and ice A plethora of hues and textures



GNP: St. Mary Prom We had an employee prom in August. Great times in St. Mary :)



Ice at One Mile Low of 22 degrees on Tuesday, December 8th, 2009.

Figure 10: **Random training samples from YFCC.**





Leather Pencil Case - Common Room PH



wiccous.com Plus Size Bottoms White / L  
Plus size cotton linen nine-point wide-leg  
pants



Arcade Belts Norrland Roark Collab Web Belt



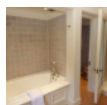
Moneta Zecchino high frypan 34 cm



social media icon set for instagram in  
different vector image



Liderazgo Educativo



manchester-bathroom-fitters-65



14 Tips for a Walt Disney World Trip with  
Tweens and Teens



Andrea Pirlo insists Juventus will not be  
resting on their 3-0 lead over Celtic



2 PC Full Bore Ball Valve



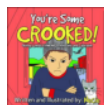
Leaves Of Fall Galaxy S5 Case



The Rise and Fall of the Trigan Empire  
Volume II



2Checkout Inline for Hikashop - enable 2nd  
address



Crooked Cover Web



Aixe Basket Club



"36" Round Solid Hardwood Dining Table Top  
(Finish Options) - UnfinishedFurnitureExpo"

Figure 11: Random training samples from LAION.



Wholesale toy candy machine for sale - Group buy The same Mini grabbing music clip candy machine small egg twisting machine grabbing childrens intellectual toys



Tug Boat Model available on Turbo Squid, the world's leading provider of digital models for visualization, films, television, and games. Tug Boats, Motor Boats, B...



Real wedding RAC Epsom on the English Wedding Blog with Murray Clarke Photography (62)



Cat smoking relax it's just the bud not corona virus vintage s Hoodie



The North Hill <PERSON> is a made in France t-shirt



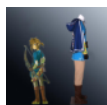
Cake on a white plate, presentation.



The swimming pool at or near Maca Villas and Spa



Weighing bananas in the supermarket. Man weighing bananas on the scales in the supermarket, close-up view with no face stock images



The Legend of Zelda Breath of The Wild Link Costume



The Green Elite Wolf Hoodie



Farmer with basket vegetables, isolated in a round frame, contour drawing, icon, logo, coloring, black and white vector. Illustration, outline cartoon drawing sto...



Students in waders stand in ocean water with a large floating net.



The Girls Rooms logo design type logo layout branding design



Each page explains an aspect of the product, with easy navigation and animation to help drive the point across.

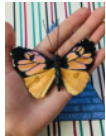


The Maze Samsung Galaxy Snap Case



Every Day Is Another Chance Sun Women's Cotton Modal Jersey Tank Dress

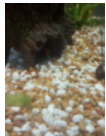
Figure 12: Random training samples from Conceptual Captions (CC-12M).



california dogface butterfly!



decent knife at a truck stop? maybe if it's from buccie's!



thought i lost my columbian spotted pleco days ago. that is till i saw this.



here is my small collection as of today



carbon



snoozy, sunny, snuggly saucissons.



these naturally forming feathers of ice.



chiquita biting more than she can chew



the living room of an industrial loft, located in an old building from 1928, in budapest, hungary. designed by golovach tatiana and andrey kot.



tapas - empanadas, potato croquettes, patatas bravas, breadsticks & melon wrapped in serrano ham, ciabatta bread with garlic butter with two types of spanish saus...



what is this mold in my basil. appeared overnight



much smaller than the rest of your creations but i decorated this cake earlier.



a newspaper i found on thanksgiving vacation. can you spot the error to?



sunrise in eastern north carolina. those aren't mountains, they are clouds



i rolled my truck last night, and found this penny while cleaning it out this morning.



the stage in the auditorium of an old high school. detroit, mi.

Figure 13: Random training samples from RedCaps.



Agathosma apiculata



Eight pence note (1778), engraved and printed by Paul Revere



Anachronous[a] map of the Dutch colonial Empire Light green: territories administered by or originating from territories administered by the Dutch East India Com...



An experiment from William Harvey's de Motu Cordis, 1628



British Army's counter-insurgency campaign in the British controlled territories of South Arabia, 1967



Deepa Shree Niraula in the left



Aerial view of Iguazu falls.



Teodor Jeske-Choński



Seymour at Wolfgang's nightclub, San Francisco, April 1987



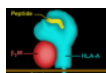
Koch at the commissioning of USS Lake Champlain in New York City, August 12, 1988



An 1862 greenback five-dollar bill



While a member of the Cleveland Indians in 1920, Elmer Smith became the first player to hit a grand slam in the World Series. He later moved down to play two seas...



HLA-A29



One of the violins in the Stradivarius collection of the Palacio Real, Madrid, Spain



Monte Cimone



Nominees Harrison and Tyler

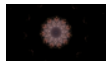
Figure 14: Random training samples from WIT.



Modern art. Colorful contemporary artwork. Color strokes of paint. Brushstrokes on abstract background. Brush painting.



Vector hand-drawn eucalyptus plant isolated on a white background



Abstract kaleidoscope background. Beautiful multicolor kaleidoscope texture. Unique kaleidoscope design.



New Year red background with Christmas balls. Vector illustration.



Greece Santorini island in Cyclades, traditional detail sights of colorful and white washed traditional houses and caldera sea in background



Happy birthday golden text on the background of red and silver gifts on a bokeh background



Friends taking a selfie at a party



Payment Failure Icon In Trendy Style Isolated Background



Summer Orchid Care



Reflections on a car parked in the street



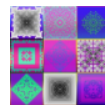
Austrian Museum of Applied Arts in Vienna, the MAK



Set of round colorful vector shapes. Abstract vector banners. Design elements. Vector illustration.



A panoramic view with village houses and cows grazing on a river bank



Abstract color background, illustration



paint colors palette with brush



Jerusalem,Israel-May 11,2018:The palmers on Holy Sepulchre Church.Anointing Unction Stone Where Jesus Body Was Wrapped Church of the Holy Sepulcher Jerusalem Isra...

Figure 15: Random training samples from Shutterstock.

## A.2 Test Distributions

Figure 16 illustrates the four distribution shifts that we use for evaluating the quality of CLIP features after pre-training on different data sources.



Figure 16: **Distribution shifts at test time.** We visualize samples of the class “broom” from the reference distribution ImageNet [19], and the four distribution shifts derived from ImageNet: ImageNet-V2 [65], ImageNet-R [36], ImageNet-Sketch [81] and ObjectNet [6].

## B Training Details

Our implementation closely follows the training code from OpenCLIP GitHub repository [38]. When training CLIP from scratch on each of the pre-training datasets, unless otherwise mentioned, we use AdamW optimizer [49] with default PyTorch parameters  $\beta_1 = 0.9, \beta_2 = 0.999, \epsilon = 10^{-8}$ , (per GPU) batch size 128 and weight decay of 0.1. For learning rate, we start with a learning rate of  $10^{-3}$  and apply a cosine-annealing learning rate schedule [48] with 5,000 steps. We use the same data augmentations as in [61]. Models then undergo distributed training on 8 A40 or A100 GPUs for 16 epochs.



## C Behavior of Individual Data Sources

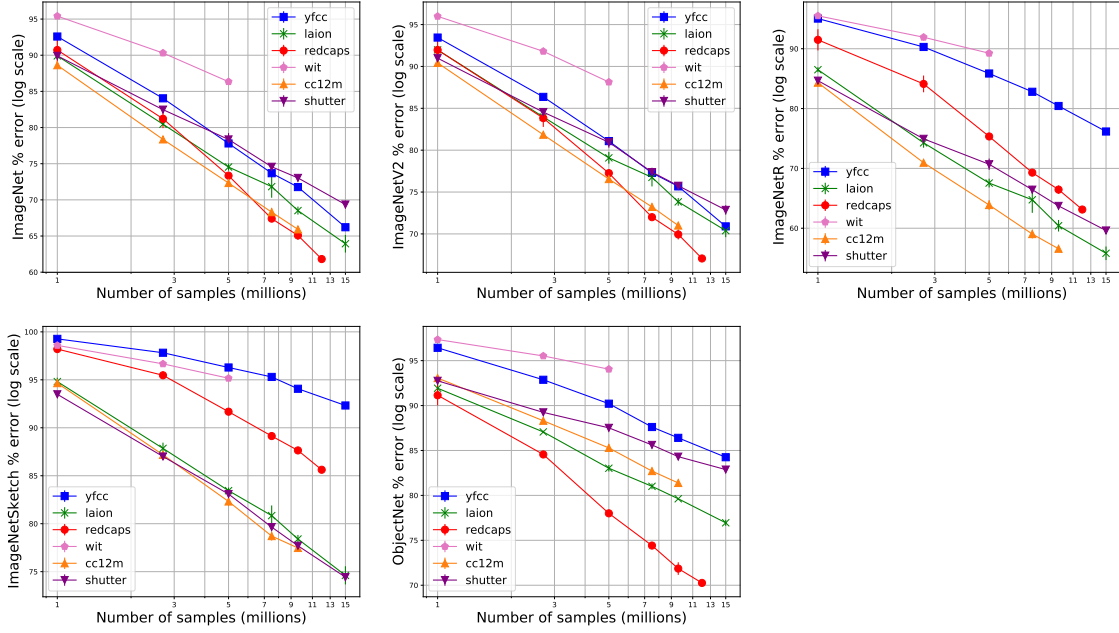


Figure 17: **Data efficiency of the six pre-training data sources on different test sets.** For each source, we randomly sample various subsets of data with sizes ranging from 1M to a maximum of 15M samples, and measure the zero-shot classification error of a CLIP model trained on the subset, on ImageNet and the four shifted test sets (i.e., ImageNet-V2, ImageNet-R, ImageNet-Sketch, ObjectNet). Plotted error values are log-transformed and averaged over 3 random seeds. We find that the data efficiency (i.e., how fast the error would decrease with more samples) of the six data sources varies significantly based on the evaluation setting.

## D Input Mixing

### D.1 More Experiments with CLIP Pre-training Data Sources

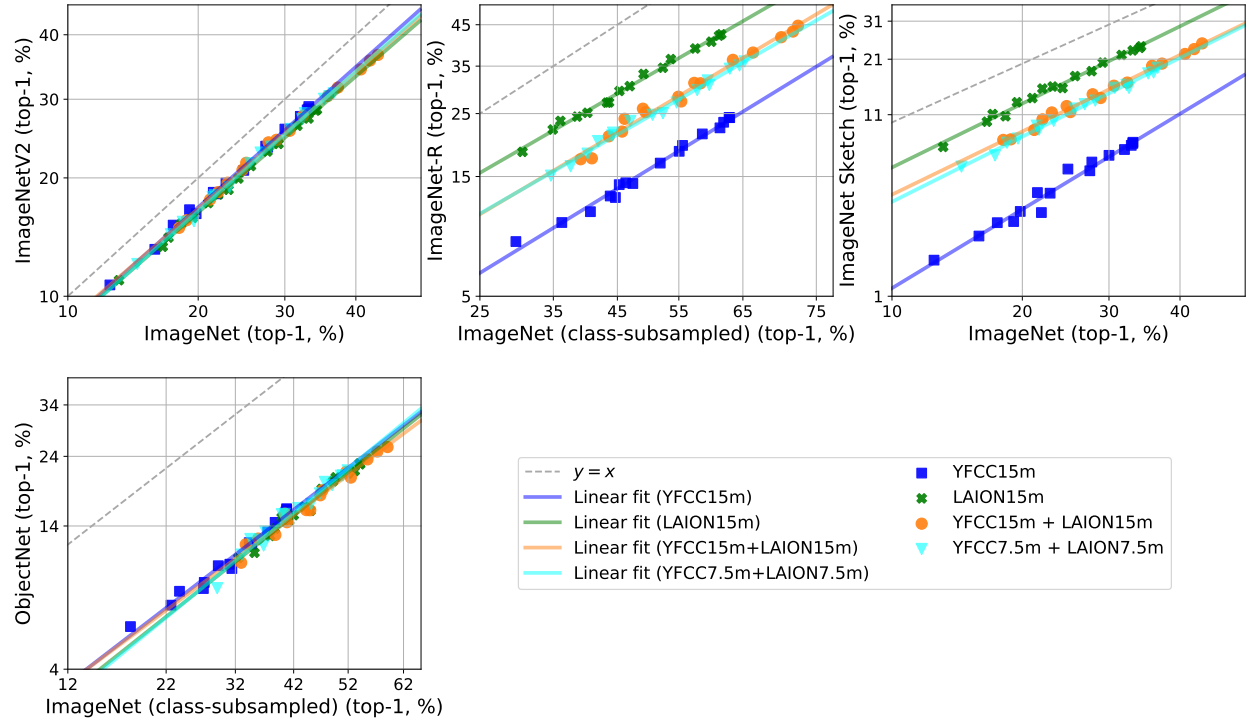


Figure 18: **Full plot for Figure 3 with all distribution shifts.** Combining YFCC and LAION training data in equal ratios results in a CLIP model with intermediate robustness.

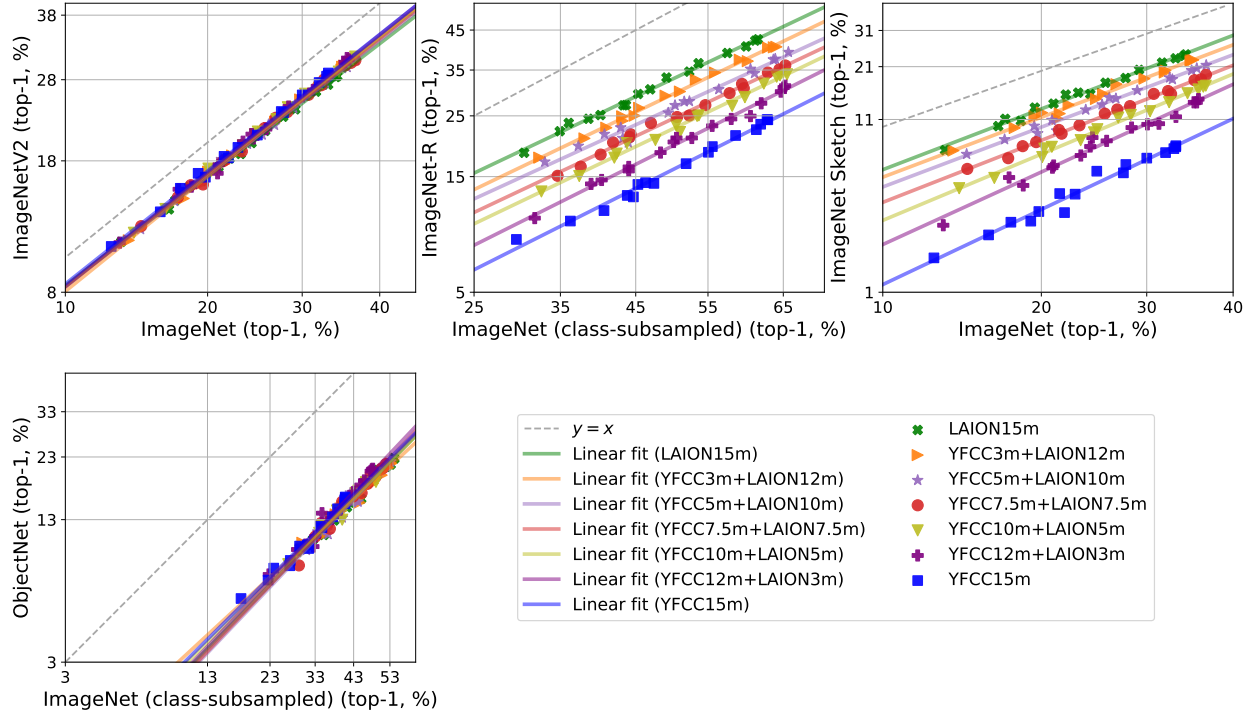


Figure 19: **Full plot for Figure 4 with all distribution shifts.** Varying the sample contributions of YFCC and LAION to the input data mixture produces a smooth interpolation of the linear trend between the trends of training on YFCC and LAION separately.

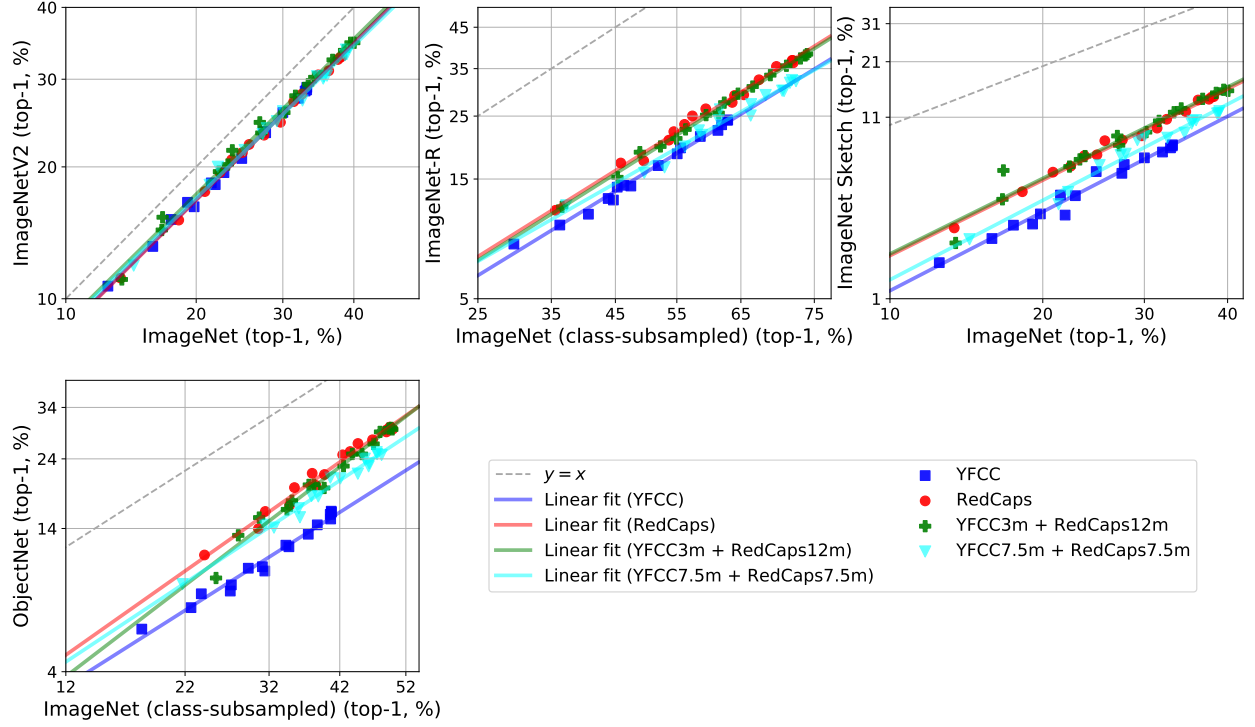


Figure 20: **Input mixing results for YFCC and RedCaps data sources.** Similar to previous observations (Figure 4), combining YFCC and RedCaps data in the pre-training dataset with different ratios yields different linear trends that all lie between that of training on YFCC and that of training on RedCaps alone.

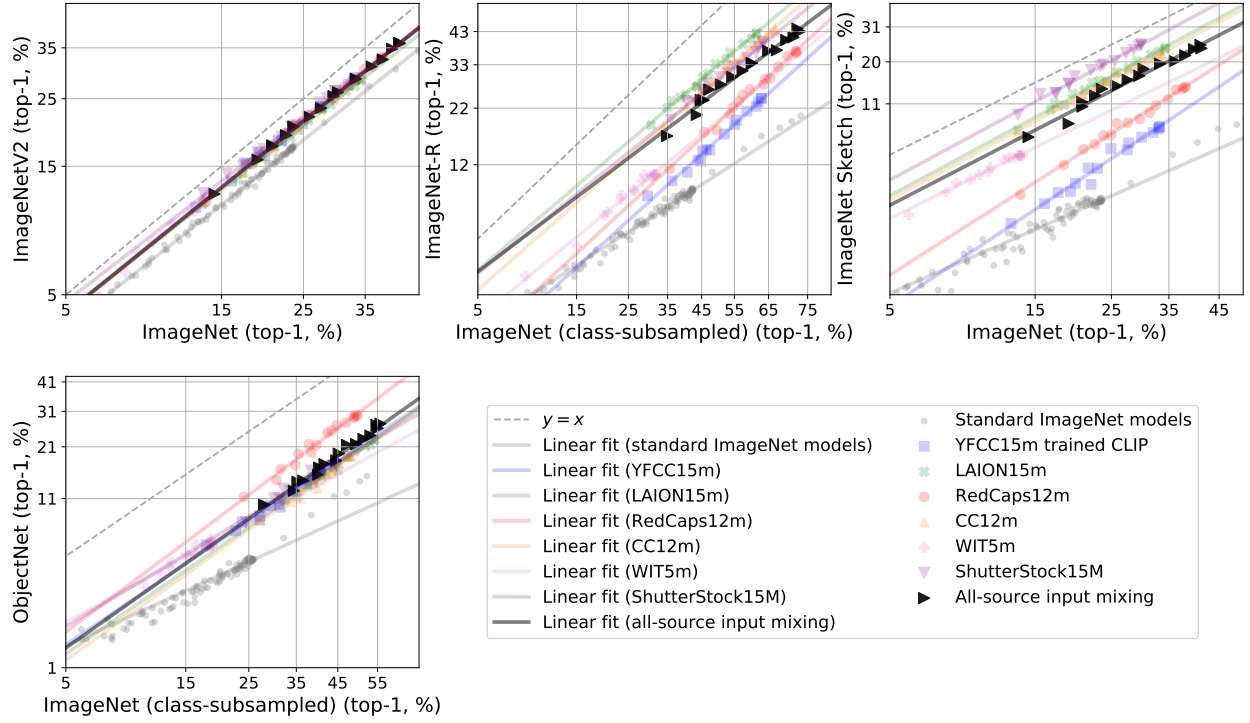


Figure 21: **Input mixing results for all six data sources.** We combine data from all six sources in the testbed with equal ratios (i.e., taking 2.7M samples from each), and find that the resulting robustness of CLIP trained on this data mixture (black line), is less than that of training only on the best-performing data source for each distribution shift setting.

## D.2 Experiments on CIFAR-10 & CINIC-10

We also investigate the phenomenon that mixing data sources resulting in diluted robustness (Section 5.1) in smaller-scale, uni-modal classification settings. Here, we experiment with mixing CIFAR-10 [43] and CINIC-10 [17] sources, each having 50K samples in total. CINIC-10 is itself a mixture of CIFAR-10 images and images selected and downsampled from the ImageNet database (for the same 10 classes). We use three architectures—ResNet-18, ResNet-34 and ResNet-50 [32]—and vary the number of epochs of training to obtain models of different accuracies. Models are evaluated on both CIFAR-10 and CINIC-10 standard test sets, and their performances are plotted along the axes of a scatter plot. Similar to previous input mixing results for CLIP, we observe in Figure 22 that ResNets trained on a 50K-sample dataset made up of *both* CIFAR-10 and CINIC-10 data, produce a linear trend that lies in between the trends of training models separately on just 50K CIFAR-10 images and just 50K CINIC-10 images.

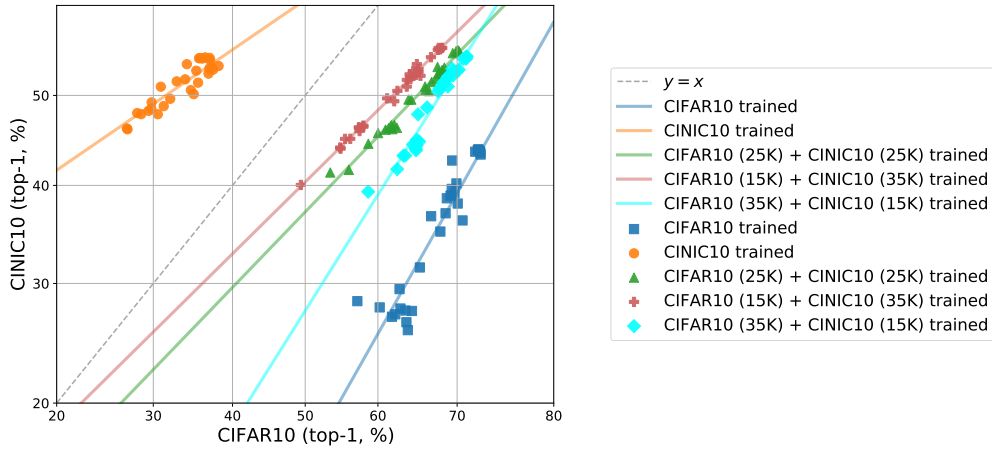


Figure 22: **Mixing inputs from CIFAR-10 and CINIC-10 distributions also produces models with intermediate robustness.** Similar to our findings from the multimodal setting with CLIP pre-training, we also observe that for standard image classification tasks like CIFAR-10 and CINIC-10, combining data samples from these two distributions with varying ratios ends up diluting the robustness of the original sources. The training set size is fixed at 50K samples for all linear trends displayed in this plot.

## E Output Mixing

### E.1 More Experiments with CLIP Pre-training Data Sources

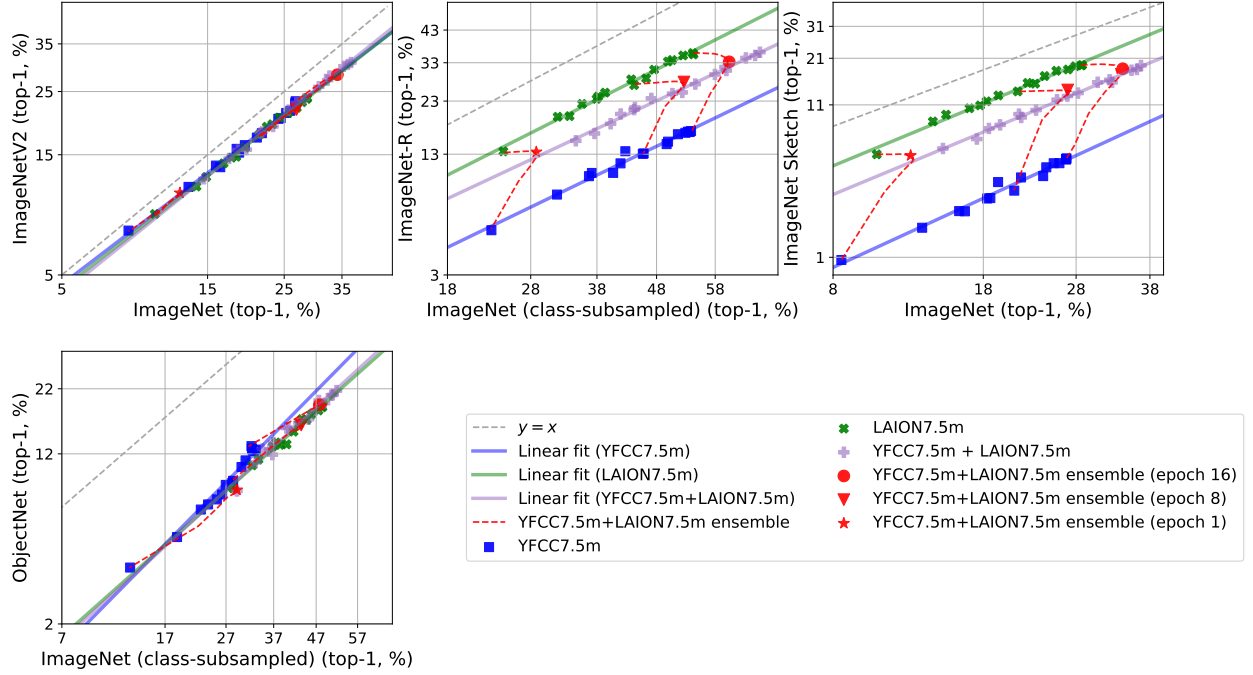


Figure 23: **Full plot for Figure 5 with all distribution shifts.** Ensemble outputs of two CLIP models trained on YFCC and LAION separately share the same linear trend as a *single* model trained on the combined data mixture (with equal sample contribution from each source).



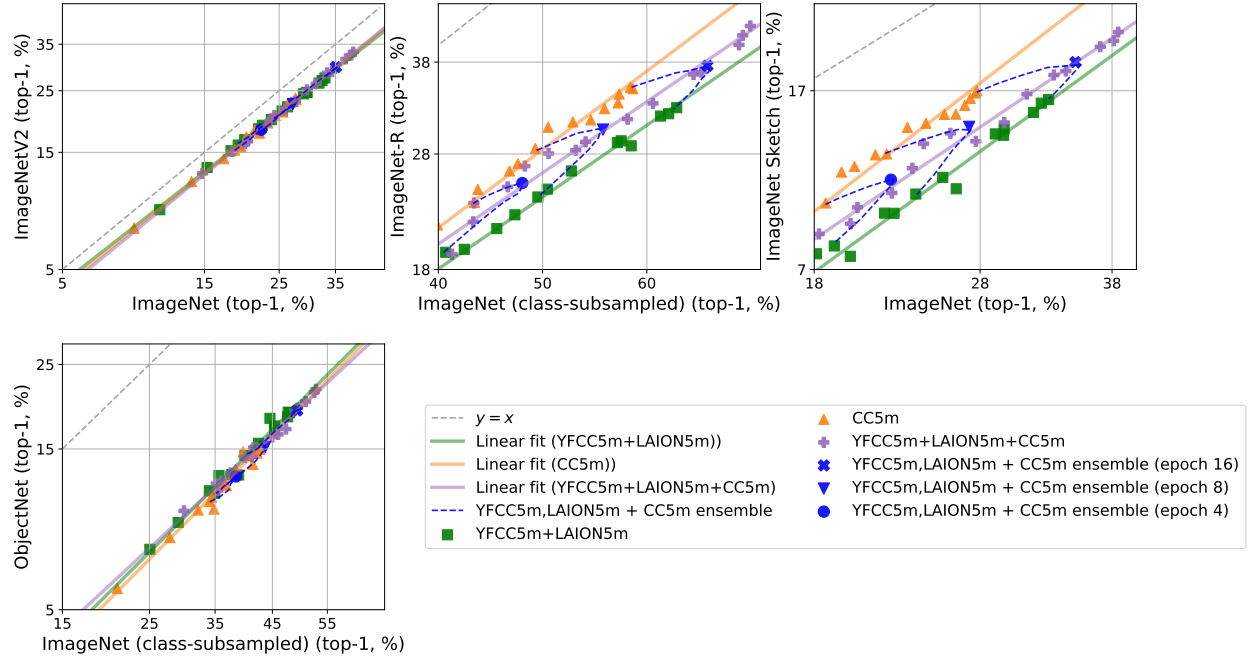


Figure 24: **Full plot for Figure 6 with all distribution shifts.** Given an existing pre-training dataset that could be a mixture (e.g., YFCC-5M + LAION-5M, green line) and a new data source (e.g., CC-5M, orange line), we could use the ensemble outputs (blue markers) of two CLIP models that have been trained separately on these two data distributions, to estimate the linear trend for models that would be trained on *all* the data (purple line).

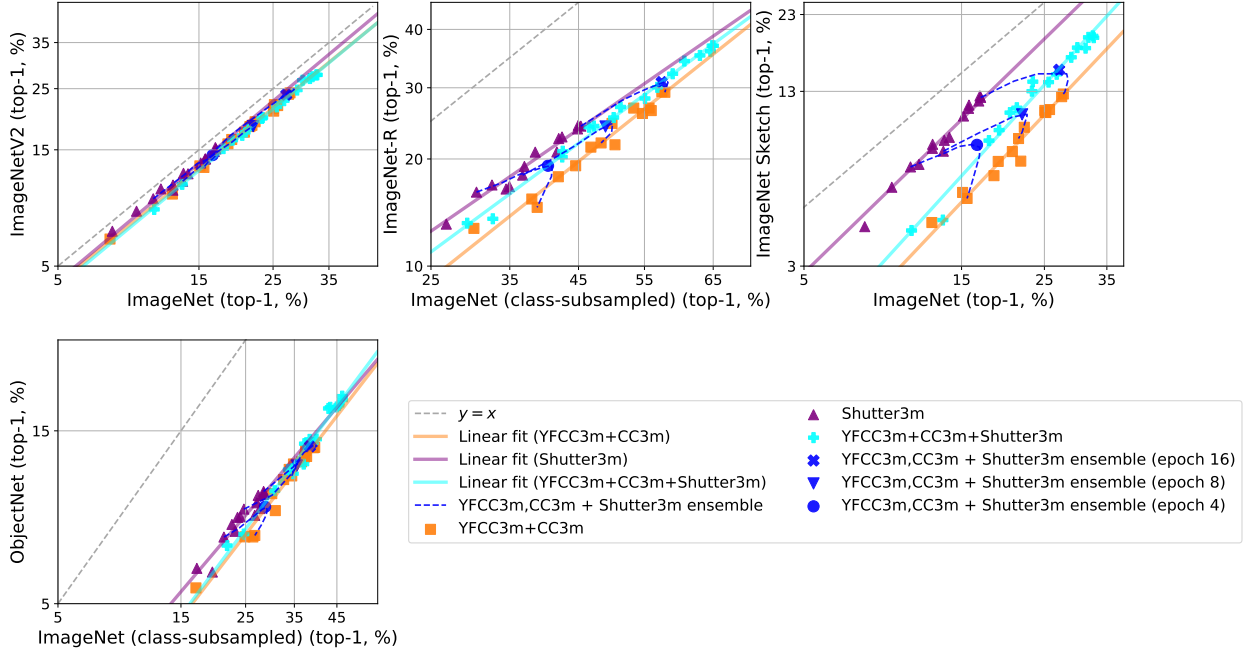


Figure 25: **Output mixing results for two CLIP models trained on YFCC-3M + CC-3M mixture and ShutterStock-3M respectively.** We repeat the experiment in Figure 24 for a different set of data sources (YFCC, ShutterStock, Conceptual Captions), taking 3M samples from each. The same output mixing phenomenon applies: the ensemble outputs of CLIPs trained on different data sources and dataset sizes (purple and orange lines), taken from the same epoch, lie on the linear trend of training a single model on the combined dataset made up of these three sources (cyan line). The two models’ logit predictions are ensembled with equal weights (blue markers).

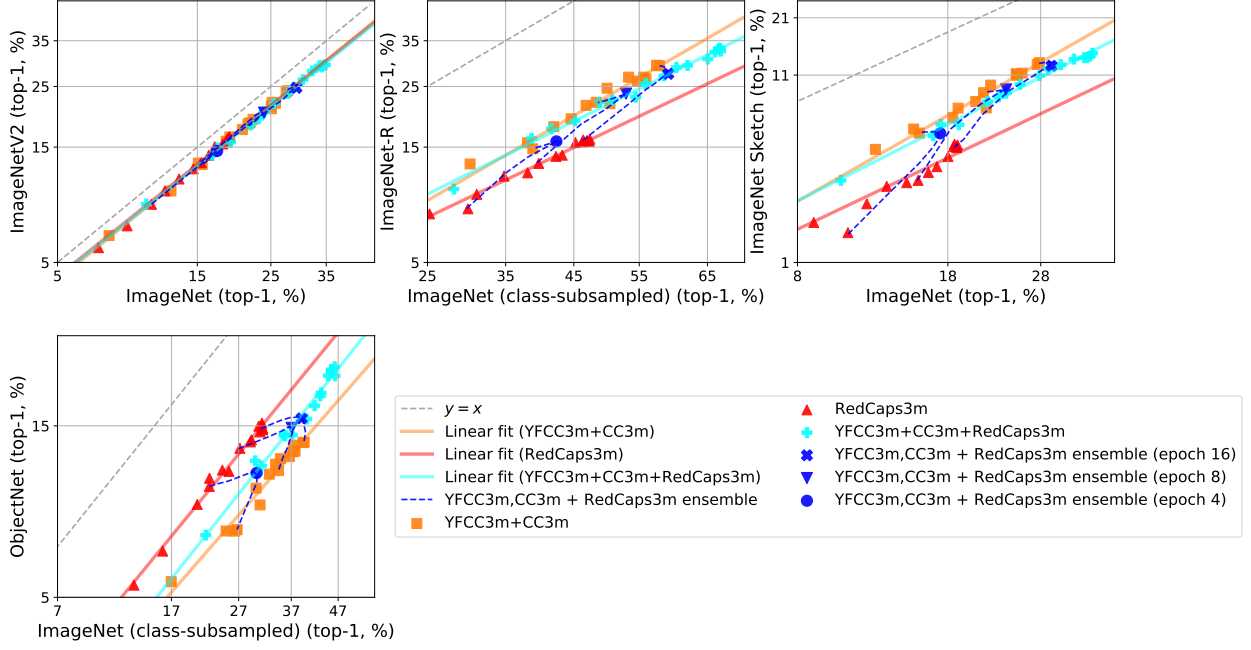


Figure 26: **Output mixing results for two CLIP models trained on YFCC-3M + CC-3M mixture and RedCaps-3M respectively.** Ensemble outputs of CLIPs trained on different data sources and dataset sizes (red and orange lines), taken from the same stage of training (i.e., epoch), lie on the linear trend of training a single model on the combined dataset made up of these three sources (cyan line), when the two models' logit predictions are ensemble with equal weights (blue markers).

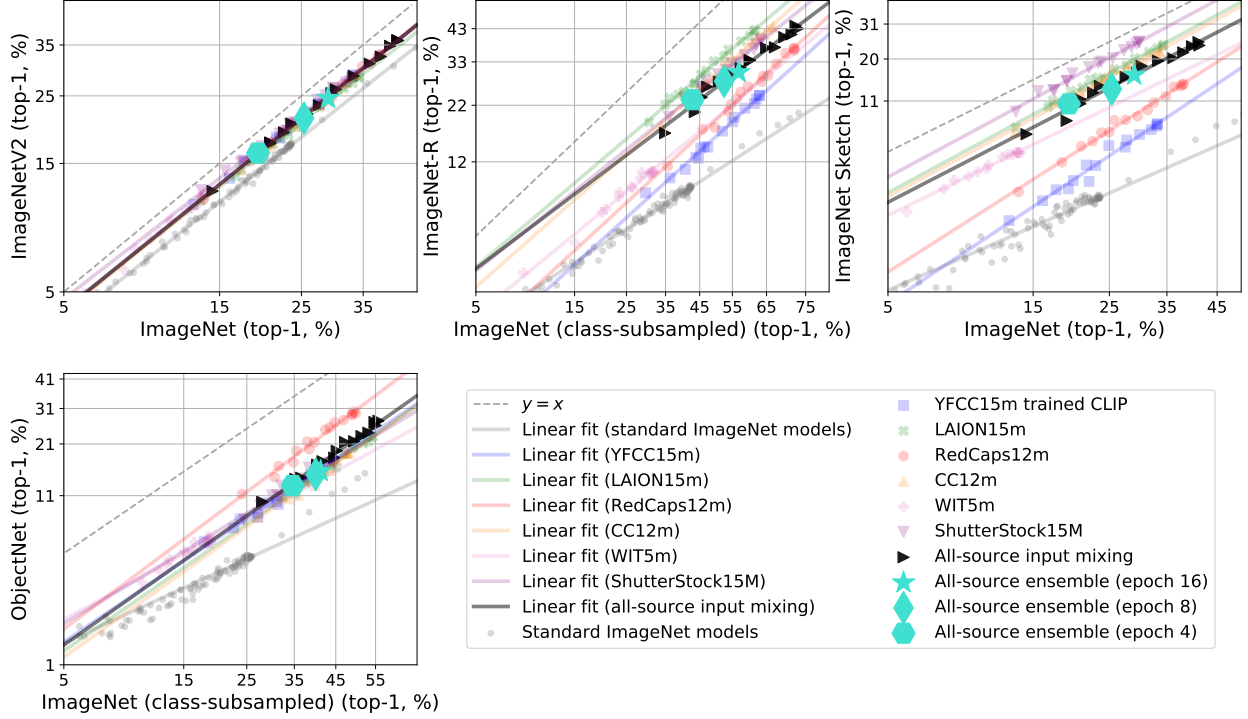


Figure 27: **Ensemble outputs of CLIPs trained separately on each of the data sources of interest share the same linear trend as a single CLIP model trained on the 6-source data mixture.** Following the input mixing setup in Figure 21, when we ensemble the logit predictions of six CLIP models, each trained on 2.7M samples randomly selected from a *single* data source, with equal weights, we find that the ensemble outputs are also predictive of the linear trend of training CLIP models on a *single* data mixture made up of 2.7M samples from each source.

## E.2 Experiments on CIFAR-10 & CINIC-10

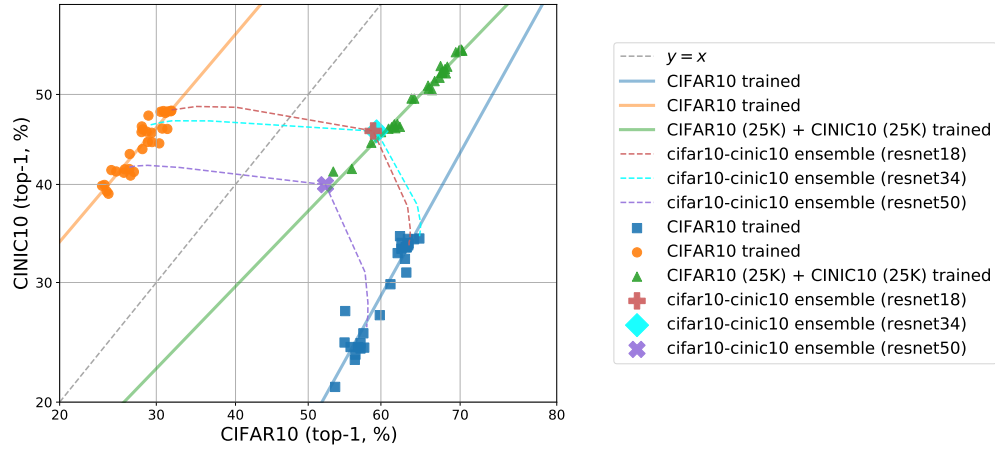


Figure 28: **Ensembling outputs of two models trained separately on CIFAR10 and CINIC10 lie on the same linear trend as training from scratch on the combined data mixture (where each source contributed equally).** We combine the logit predictions of CINIC10-trained and CIFAR10-trained models that have the same architecture (e.g., ResNet-18, ResNet-34 and ResNet-50 in this case) with varying ensemble weights between 0 and 1 (dashed lines). Similar to our findings from the multimodal setting with CLIP, we also observe that when the predictions are combined with equal weights (markers on the dashed lines), the resulting test accuracies on the two corresponding test sets lie on the linear trend produced by training ResNets on a  $\text{CIFAR10} + \text{CINIC10}$  data mixture with equal number of samples from each source.

## F Proofs of the Analyses

We provide proofs of main theoretical claims in Section 6.

### F.1 Proof of Theorem 1

**Assumption 5.** *Under the hypotheses of Theorem 1, suppose there exists a positive constant  $c$  such that the third moments are bounded by  $\mathbb{E}_{(X,Y) \sim P_{\theta_1, \rho_1}}[(X_i Y - \theta_{1,i})^3] \leq c \mathbb{E}_{(X,Y) \sim P_{\theta_1, \rho_1}}[(X_i Y - \theta_{1,i})^2]^{3/2}$ ,  $\mathbb{E}_{(X,Y) \sim P_{\theta_2, \rho_2}}[(X_i Y - \theta_{1,i})^3] \leq c \mathbb{E}_{(X,Y) \sim P_{\theta_2, \rho_2}}[(X_i Y - \theta_{1,i})^2]^{3/2}$ , and  $\mathbb{E}[(\hat{\theta}_{n,i} - \theta_i)^3] \leq c \mathbb{E}[(\hat{\theta}_{n,i} - \theta_i)^2]^{3/2}$  for all  $i \in [d]$ .*

Under this assumption, we show that

$$\Phi^{-1}(\text{Acc}_{\theta_1, \rho_1}) = \cos(\theta_1, \theta) \rho_1 \frac{\rho}{\xi} \sqrt{\frac{n}{d}} + O\left(\frac{\exp(\frac{\rho_1^2 \rho^2 n}{2\xi^2 d})}{\sqrt{n}}\right), \text{ and} \quad (4)$$

$$\Phi^{-1}(\text{Acc}_{\theta_2, \rho_2}) = \cos(\theta_2, \theta) \rho_2 \frac{\rho}{\xi} \sqrt{\frac{n}{d}} + O\left(\frac{\exp(\frac{\rho_2^2 \rho^2 n}{2\xi^2 d})}{\sqrt{n}}\right), \quad (5)$$

as it will make the first and second claims straightforward. For  $(X_1, Y_1) \sim P_{\theta_1, \rho_1}$ , the first error event is  $\{\text{sign}(\langle X_1, \hat{\theta}_{n, \xi} \rangle) \neq Y_1\} = \{\langle X_1, \hat{\theta}_{n, \xi} \rangle Y_1 \leq 0\} = \{\langle \theta + (\xi \|\theta\| / \rho \sqrt{n}) z, \theta_1 + (\|\theta_1\| / \rho_1) z_1 \rangle \leq 0\}$ , where we used the fact that  $\hat{\theta}_{n, \xi} = \theta + (\xi \|\theta\| / \rho \sqrt{n}) z$  and  $XY \stackrel{d}{=} \theta_1 + (\|\theta_1\| / \rho_1) z_1$ . Since the third moments are bounded, applying Berry-Esseen theorem, we get that the probability of error is bounded by  $\Phi(-(\langle \theta, \theta_1 \rangle \rho_1 \rho \sqrt{n} / (\xi \|\theta_1\| \|\theta\| \sqrt{d}))) + O(1/\sqrt{d})$ . This gives  $\text{Acc}_{\theta_1, \rho_1} = \Phi(\langle \theta, \theta_1 \rangle \rho_1 \rho \sqrt{n} / (\xi \|\theta_1\| \|\theta\| \sqrt{d})) + O(1/\sqrt{d})$ , and consequently

$$\Phi^{-1}(\text{Acc}_{\theta_1, \rho_1}) = \cos(\theta_1, \theta) \rho_1 \frac{\rho}{\xi} \sqrt{\frac{n}{d}} + O\left(\frac{e^{\frac{\cos(\theta_1, \theta)^2 \rho_1^2 \rho^2 n}{2\xi^2 d}}}{\sqrt{n}}\right). \quad (6)$$

This proves the desired claim.

### F.2 Proof of Theorem 2

Recall that  $\text{Slope}(\hat{\theta}_n(\mathcal{D}_{n, \theta, \rho})) = c \langle \theta_2, \theta \rangle / \langle \theta_1, \theta \rangle$  for a positive constant  $c > 0$  that does *not* depend on the training data. Although the slope only depends on the training data and algorithm through  $\theta$ , we write all the parameters including the sample size  $n$  and the training SNR  $\rho$  to make it explicit that the results hold for all variations of the sample size and the training algorithm within the class that we assume. It is sufficient to show that this is a monotonic function over  $\theta$  when we linearly traverse from  $\tilde{\theta}_1$  to  $\tilde{\theta}_2$ , i.e.  $\theta(\alpha) = \alpha \tilde{\theta}_1 + (1 - \alpha) \tilde{\theta}_2$  for  $\alpha \in [0, 1]$ . Note that  $f(\alpha) = c \langle \theta_2, \theta(\alpha) \rangle / \langle \theta_1, \theta(\alpha) \rangle = c_1 + c_2 / \langle \theta_1, \theta(\alpha) \rangle$  for some  $c_1$  and  $c_2$  that do not depend on  $\alpha$ . The monotonicity follows from the fact that the derivative is

$$\frac{\partial f(\alpha)}{\partial \alpha} = -c_2 \frac{\langle \theta_1, \tilde{\theta}_1 - \tilde{\theta}_2 \rangle}{\langle \theta_1, \theta(\alpha) \rangle^2},$$

whose sign does not change for any  $\alpha$ .

### F.3 Proof of Theorem 3

The train data distribution satisfies  $x_i y_i \sim \mathcal{N}(\theta_{\text{train}}, (\|\theta_{\text{train}}\|/\rho)^2 \mathbf{I})$ . Note that filtering does not change the distribution in  $d - 1$  dimensional subspace orthogonal to  $\hat{\theta}_{\text{pretrained}}$ , due to rotation invariance of a spherical Gaussian distribution. This implies that  $\mathbb{E}[\mathcal{P}_{\perp}(\hat{\theta}_{\text{filtered}})] = \mathcal{P}_{\perp}(\theta_{\text{train}})$ , where  $\mathcal{P}_{\perp}$  denotes the projection operator to the  $d - 1$  dimensional subspace orthogonal to  $\hat{\theta}_{\text{pretrained}}$ . On the other hand, on the direction of  $\hat{\theta}_{\text{pretrained}}$ , the filtering increases the correlation in expectation:  $|\mathbb{E}[\mathcal{P}_{\parallel}(\hat{\theta}_{\text{filtered}})] - \mathcal{P}_{\parallel}(\hat{\theta}_{\text{pretrained}})| \leq |\mathcal{P}_{\parallel}(\theta_{\text{train}}) - \mathcal{P}_{\parallel}(\hat{\theta}_{\text{pretrained}})|$ , where  $\mathcal{P}_{\parallel}$  denotes the projection operator to the one dimensional subspace spanned by  $\hat{\theta}_{\text{pretrained}}$ . This implies that  $\mathbb{E}[\hat{\theta}_{\text{filtered}}] = \theta_{\text{train}} + c\hat{\theta}_{\text{pretrained}}$  for some positive  $c$ . It follows that  $\mathbb{E}[\hat{\theta}_{\text{filtered}}]$  is a convex interpolation between two vectors, each in the direction of  $\theta_{\text{train}}$  and  $\hat{\theta}_{\text{pretrained}}$ , respectively. We can apply Theorem 2 which gives that

$$\text{Slope}(\hat{\theta}_{\text{unfiltered}}) < \text{Slope}(\mathbb{E}[\hat{\theta}_{\text{filtered}}]) \leq \text{Slope}(\hat{\theta}_{\text{pretrained}}),$$

when  $\text{Slope}(\hat{\theta}_{\text{unfiltered}}) < \text{Slope}(\hat{\theta}_{\text{pretrained}})$ .